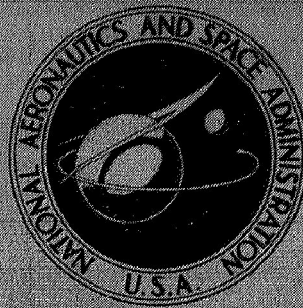


NASA TECHNICAL
MEMORANDUM



NASA TM X-3011

NASA TM X-3011

CASE FILE
COPY

WIND TUNNEL BLOCKAGE AND
SUPPORT INTERFERENCE EFFECTS
ON WINGED-BODY MODELS AT
MACH NUMBERS FROM 0.6 TO 1.0

by Bernard J. Blaha
Lewis Research Center
Cleveland, Ohio 44135

1. Report No. NASA TM X-3011	2. Government Accession No.	3. Recipient's Catalog No.	
4. Title and Subtitle WIND TUNNEL BLOCKAGE AND SUPPORT INTERFERENCE EFFECTS ON WINGED-BODY MODELS AT MACH NUMBERS FROM 0.6 TO 1.0		5. Report Date MARCH 1974	
		6. Performing Organization Code	
7. Author(s) Bernard J. Blaha		8. Performing Organization Report No. E-7596	
		10. Work Unit No. 501-24	
9. Performing Organization Name and Address Lewis Research Center National Aeronautics and Space Administration Cleveland, Ohio 44135		11. Contract or Grant No.	
		13. Type of Report and Period Covered Technical Memorandum	
12. Sponsoring Agency Name and Address National Aeronautics and Space Administration Washington, D. C. 20546		14. Sponsoring Agency Code	
		15. Supplementary Notes	
16. Abstract <p>Three sting-mounted winged-body models with tunnel blockages of 0.1, 1.0, and 2.0 percent were tested in the Lewis Research Center's 8- by 6-Foot Supersonic Wind Tunnel. Fuselage pressures were obtained over a Mach number range of 0.6 to 1.0 at angles of attack from 0° to 4°. Two other types of model support were investigated, which included simulated wing-tip and fuselage support-strut mountings. The effects of tunnel porosity and sidewall geometry were also investigated. Model blockage effects were small up to $M_0 = 0.95$. At higher speeds the major blockage effect observed was a displacement of the local transonic terminal shocks on the model. The effects of the wing-tip type of model support were small up to $M_0 = 0.95$, but disturbances were observed on the fuselage at higher speeds. Changes in local tunnel porosity were effective in reducing the disturbances up to $M_0 = 0.975$, but a change in sidewall geometry was not.</p>			
17. Key Words (Suggested by Author(s)) Transonic; Blockage ratio; Support interference; Tunnel wall interference; Model support; Winged body; Near sonic		18. Distribution Statement Unclassified - unlimited	
19. Security Classif. (of this report) Unclassified		20. Security Classif. (of this page) Unclassified	22. Price* \$3.00
		21. No. of Pages 36	Cat. 01

* For sale by the National Technical Information Service, Springfield, Virginia 22151

WIND TUNNEL BLOCKAGE AND SUPPORT INTERFERENCE EFFECTS ON WINGED-BODY MODELS AT MACH NUMBERS FROM 0.6 TO 1.0

by Bernard J. Blaha
Lewis Research Center

SUMMARY

Tests were conducted in the Lewis Research Center's 8- by 6-Foot Supersonic Wind Tunnel to investigate the effects of model blockage and support interference with several sizes of winged-body configurations. To determine interference effects, fuselage pressures were compared for three sting-mounted models, which included maximum model cross-sectional area to test-section area ratio of 0.1, 1.0, and 2.0-percent. Also, an axisymmetric 0.1-percent blockage model was tested for reference. Two other types of model support were investigated, which included wing-tip and fuselage support-strut mountings. The effects of tunnel porosity and tunnel sidewall geometry were also investigated. Data were obtained over a Mach number range of 0.6 to 1.0 at angles of attack from 0° to 4° .

Axisymmetric model results indicate that tunnel blockage effects were small up to free-stream Mach number $M_0 = 0.975$. With the winged-body models blockage effects were small up to $M_0 = 0.95$. In both cases the predominant blockage effect seen at the higher Mach numbers was a displacement of the local transonic terminal shocks on the model. The effects of a wing-tip type of model support were small up to $M_0 = 0.95$, but at higher Mach numbers a disturbance was generated aft on the model. Changes in tunnel local porosity, however, reduced this disturbance up to $M_0 = 0.975$. A change in tunnel sidewall geometry was not effective. The effects of a forward fuselage swept support-strut were small.

INTRODUCTION

Recent studies have been made to investigate the problems associated with the development of an advanced near sonic transport (refs. 1 to 4 and three unpublished reports on work performed at the NASA Langley Research Center by R. A. Langhans and

R. T. Whitcomb, by S. G. Flechner, and by L. W. McKinney, J. F. Herman, and L. A. Bodin). One of the more significant problems for this type of aircraft that is presently being investigated at Lewis is the integration of the propulsion system with the airframe (ref. 4). One of the major reasons present transport aircraft do not cruise at higher speeds is the interference drag resulting from the interaction of the propulsion system and airframe flow fields. Therefore, the selection of the proper engine nacelle design and its position on the airframe is an important factor in attempting to increase cruise speed (refs. 4 to 8). It is also important that the airframe flow field not cause adverse conditions for the propulsion system components.

As a direct result of this work a renewed emphasis has been made to obtain accurate pressure and drag data in wind tunnels at near sonic speeds ($M_0 = 0.9$ to 1.0). To properly evaluate the interactions between the propulsion system and the airframe at these speeds, it is imperative that the flow field in the wind tunnel be correct and that the wall and model support interference effects be a minimum. Previous results obtained from numerous transonic wind tunnel tests have indicated that wall interference and model support interference effects can significantly influence model pressures and resulting drag especially at near sonic speeds. References 9 to 13 describe several studies that were conducted to determine model blockage and support interference effects with axisymmetric models. The results of references 9 and 10 indicate that significant wind tunnel blockage effects occur on the drag of a series of various sized axisymmetric models for Mach numbers above 0.96, even with model blockages as small as 0.03 percent. Similar effects are seen in the results reported in references 11 and 12, and reference 13 describes the effects of several types of model support on axisymmetric model pressures and afterbody drag.

To further investigate some of these effects on winged-body configurations, a series of tests were conducted in the Lewis Research Center's 8- by 6-Foot Supersonic Wind Tunnel with several values of model blockage. Fuselage pressures were measured and are presented herein for three sting-mounted winged-body models. These models had values of ratio of maximum model cross-sectional area to test-section area (or blockage) of 0.1, 1.0, and 2.0 percent. Data were obtained over a Mach number range from 0.6 to 1.0 at angles of attack from 0° to 4° . Other model support methods for the 1.0-percent model were investigated, which included simulated wing-tip mounting and a lower fuselage forward swept support strut. The effects of variations in local tunnel wall porosity and local tunnel sidewall geometry were also investigated. A 0.1-percent blockage axisymmetric model was also tested for reference, and the results are compared with previous test results in another facility.

SYMBOLS

A	cross-sectional area of model
A_{\max}	maximum cross-sectional area of model
b	wing span
C_p	pressure coefficient $(p - p_0)/q_0$
$C_{p_{\text{sonic}}}$	pressure coefficient corresponding to $M = 1.0$ local flow
c	wing chord
L	model length
M_0	free-stream Mach number
p	local static pressure
p_0	free-stream static pressure
q_0	free-stream dynamic pressure
R	radial distance coordinate
r	radius length
X	axial distance coordinate along model
α	model angle of attack, deg
φ	angular position coordinate, deg

APPARATUS AND PROCEDURE

Figure 1 is a schematic drawing of the installation of the models in the transonic test section of the Lewis 8- by 6-Foot Supersonic Wind Tunnel. The models were all sting-mounted from the tunnel floor strut. Because of its large size, the nominally 2-percent blockage model had its wings cut off at the intersection with the tunnel side-walls (thereby slightly reducing its blockage). The location of the base of all the models was maintained at a single tunnel station. This station was selected based on the results of references 11 and 12 to be far enough upstream of a flow acceleration region that exists in the aft portion of the transonic test section. This is of particular concern for aft fuselage engine nacelle installations. This base location was 1.201 meters from the end of the perforated test section. Tests were conducted over a range of Mach numbers from 0.6 to 1.0 at angles of attack from 0° to 4° . Reynolds numbers varied from 12.25×10^6 per meter at Mach 0.6 to 15.0×10^6 per meter at Mach 1.0. The 0.1-percent

and 1.0-percent blockage models were tested in the modified 2.44-meter (8-ft) test section with 3.1-percent porosity. Because of its length, the 2-percent model, however, had to be tested in the 4.27-meter (14-ft) test section with 5.8-percent porosity. During the testing some local variations in the tunnel porosity in the wing-tip region were investigated.

A schematic drawing of the axisymmetric model is shown in figure 2. Instrumentation locations (fig. 2(a)) and a photograph of the model in the tunnel (fig. 2(b)) are also shown. This model was a parabolic design with an overall model length-to-diameter ratio (fineness ratio) of 10. Coordinates (fig. 2(a)) were scaled from those of the model described in reference 14. The model was scaled such that it resulted in a tunnel blockage at a 0° angle of attack of 0.1 percent. This resulted in a model that was 64.3 centimeters long with a maximum diameter of 7.587 centimeters. The same ratio of sting diameter to maximum model diameter as was used in reference 14 was used in this test so that the data could readily be compared between the two separate tests. Because of the sting support, the actual geometric model fineness ratio was only 8.48 (to the juncture with the sting). The model was instrumented as shown in figure 2(a) with a row of pressure orifices along the top. Three other rows of scattered orifices were installed for alinement reference. The purpose of this reference model was to provide a set of low blockage data that could be compared with data from another facility and with theoretical calculations.

The three winged-body models tested were designed so that the sum of the cross-sectional area distributions of the individual components (fuselage, wing, and wing gloves) matched that of an axisymmetric body, which has demonstrated low drag characteristics at speeds near $M_0 = 1.0$. This body has a ratio of model length to maximum diameter of about 9.5. The resulting area distribution of the winged-body models is shown in figure 3. In the region of the wings the total area distribution was compensated for the supersonic stream-tube expansion associated with the supercritical flow over the wings. This is the reason for the depressed region just aft of the maximum area. The details of the winged-body models are shown in figure 4. Three sizes of model were tested, which included maximum tunnel blockages at a 0° angle of attack of 0.1, 1.0, and 2.0 percent. The dimensions of the three models and instrumentation locations are shown in figure 4(a). Photographs of the three sizes of model mounted in the tunnel are shown in figures 4(b) to (e). The models were sting mounted and were made up of three separate components: the fuselage, the wing, and the wing gloves. The variation in blockage size from 0.1 to 2.0 percent resulted in model lengths of 66.5, 210.1, and 297.9 centimeters. Each of the larger stings were scaled from the 0.1-percent blockage model.

The fuselage was an axisymmetric design that was contoured to provide area ruling in the region of the wing. The wing was a symmetrical airfoil with leading and trailing

edge sweep back angles of 44.5° and 35° , respectively. These angles would be typical for a transport designed to cruise at near sonic speeds. The wing semispan lengths were 42 percent of the fuselage length except for the 2.0-percent model, whose wing had to be truncated at 70-percent semispan because of the limiting width of the tunnel test section. The symmetrical airfoil section was made up of simple geometric shapes (circular arc leading edges, trapezoidal intermediate sections, and triangular shaped trailing edge) so that it could be fabricated easily and inexpensively. The wing chord diminished from 16.72-percent of the fuselage length at the root to 6.83-percent of the fuselage length at the tip.

As can be seen in figure 3 a large area deficiency would exist in the model area distribution if only the fuselage and wing were present. Therefore, to smooth out this deficiency, simulated wing gloves were added to the models. These also were made up of simple geometric shapes. The leading and outboard edges were semicircular and the leading edge had a sweep back angle of 54° . The glove cross section was rectangular in the streamwise direction and trapezoidal in the spanwise direction such that it blended with the wing leading edge and diminished in thickness with increasing semispan. The width of the gloves was 37 percent of the wing semispan. To determine the effects of the presence of the gloves on the fuselage pressures, the 0.1-percent blockage model was tested both without and with the wing gloves as seen in figures 4(b) and (c), respectively.

The models were instrumented with three rows of static-pressure orifices located on the fuselage top, side, and bottom. Extra statics were distributed along the aft side of the model in the region where an aft-fuselage engine nacelle might be located on a full-scale transport.

Also shown in figure 4(a) are constant section wing panels that were tested on the 1.0-percent blockage model. These panels were sheet metal covers that converted the wing into a constant cross section wing from either the 37- or 70-percent semispan location to the wing tip. These wing panels were tested to evaluate the interference associated with thickened wings. If a model like this was supported by wing-tip mounts, the outboard part of the wings would have to be thickened to maintain structural integrity. Therefore, it was desired to determine what effect such a modified wing would have on the aft fuselage pressures.

A schematic drawing showing the relative sizes of the three winged-body models tested is shown in figure 5. As mentioned previously all the models were located with the model base at the same tunnel axial station. The 1.0-percent blockage model was tested both clean and with the simulated constant section wing. The 2.0-percent model as shown in both figures 4 and 5 had shortened wings because of the limiting width of the tunnel test section.

Photographs of the 1.0-percent blockage model with the simulated constant section

wing panels are shown in figure 6. Figure 6(a) shows the panels at the 0.7 semispan station, and figure 6(b) shows them at the 0.37 semispan station. As will be shown in the RESULTS AND DISCUSSION, the constant section wing did produce an adverse effect on the fuselage pressures at speeds near Mach 1.0. Therefore, an attempt was made to compensate for these effects by altering the porosity of the tunnel sidewall in the vicinity of the wing. This can be seen in figure 6(b). Another method was also tested in which the tunnel sidewalls were determined is shown in figure 7.

A 53.4-centimeter high section of the tunnel sidewall was removable and was replaced with a contoured plate. The contour was designed so that it nearly compensated for the added blockage area distribution generated by the constant section wing panels. Details of the contoured wall section are shown in figures 7(a) and (b), and photographs are shown in figures 7(c) and (d).

The effects of a forward fuselage swept strut model support were also investigated with the 1.0-percent blockage model. Details of a simulated strut that was tested are shown in figure 8. A thin ($t/c = 0.0965$ stream-wise direction) simulated strut was installed from the underside of the forward fuselage. To minimize the axial buildup of blockage, the simulated strut had a 45° sweep angle. The cross section again was made up of simple geometric shapes (semicircular leading edge, rectangular center-section, and 15° triangular trailing edge). Details of the installation are shown in figure 8(a) and a photograph of the installation in the test section is shown in figure 8(b).

Boundary-layer trips were installed on the fuselage and the upper and lower surfaces of the wings and gloves. A 0.76-centimeter strip of No. 80 grit was used in all cases. Transition was fixed at $0.05 L$ on the fuselage and at about $0.1 c$ on the wing and glove surfaces.

RESULTS AND DISCUSSION

Pressure distributions on the 0.1-percent axisymmetric blockage model are presented in figure 9. Data are presented over a Mach number range from 0.6 to 1.0 at a 0° angle of attack. These data indicate no significant disturbances up to Mach 0.975. At Mach 1.0 a disturbance is apparent on the aft portion of the model beginning at axial station $X/L = 0.75$. The abruptness of the pressure rise indicates the presence of a shock. The presence of the shock at this location is probably the combined result of two effects: the presence of the sting and a blockage effect resulting in a retardation of this transonic terminal shock. As indicated in references 9 and 10, a 0.1-percent blockage is large enough to result in significant blockage effects at Mach 1.0. The most significant result is seen as a retardation of the passage of the transonic terminal shock over the model (refs. 11 and 12).

A comparison of axisymmetric 0.1-percent blockage model pressure distributions with theoretical predictions and data from a geometrically similar 0.2-percent blockage model tested in another facility (ref. 14) is presented in figure 10. Comparisons are made over a Mach number range from 0.8 to 1.0 at a 0° angle of attack. The theoretical predictions were calculated using the local linearization theory method presented in reference 15. The 0.1-percent model coordinates were scaled from the model described in reference 14 with a fineness ratio of 10. Therefore, the data obtained in the Ames Research Center's 14-Foot Transonic Tunnel could be directly compared with the present results. The agreement between the two sets of model data was excellent except at Mach 1.0, where slight differences were observed in the disturbance on the aft region of the model. These slight differences could be the result of the differences in model blockage or possibly of small differences in model contour. Both sets of data agree well with the theoretical predictions except where there were regions of supercritical flow. These results indicate that the blockage effects in the tunnel are generally small up to $M_0 = 0.975$ for an axisymmetric model of this size and also that there are no other inherent tunnel generated or reflected disturbances.

Pressure distributions on the 0.1-percent blockage winged-body model are presented in figure 11. Data are presented for a Mach number range of 0.6 to 1.0 at a 0° angle of attack. Since this was the smallest blockage winged model the data from this model was considered to be the reference. As can be seen in figure 11 the area-ruled geometry of the fuselage results in two expansions and recompressions. Between Mach 0.95 and 1.0 these recompressions become very abrupt and since, as indicated by the $C_{P, \text{sonic}}$ designations, the flow just upstream is supercritical, these recompressions are probably terminal shocks. Also, as is indicated by the results of references 9 and 10, they are probably displaced at a given Mach number from where they would be if there were no blockage.

A comparison of the pressure distributions on the 0.1-, 1.0-, and 2.0-percent blockage models is shown in figure 12. Data are presented over a range of Mach numbers from 0.6 to 1.0 at a 0° angle of attack. Fairly good agreement can be seen up to Mach 0.95, except for some small disagreements near the nose of the models and at a few stations along the body. These small disagreements, as will be demonstrated later, are probably the result of small differences in the model contour between the various sized models. At Mach 0.95 and above significant differences in the data become apparent especially near model axial stations $X/L = 0.4$ and 0.8 . These are the same locations the transonic terminal shocks were noted on the small model at these same speeds. As can be seen in figure 12, the first shock is displaced upstream with increasing blockage. The opposite trend seems to occur for the aft terminal shock when it is displaced aft with increasing blockage. In general, the most significant displacement in both cases seems to occur when the blockage is increased from 0.1 to 1.0 percent. A

further increase in blockage to 2.0 percent generally results in only a small additional displacement of these shocks. These results agree with the results of references 9 to 12 in that the most significant tunnel blockage effect seen at these speeds is a displacement of the transonic terminal shock with increasing tunnel blockage. It is evident, then, that reasonable data free of tunnel blockage effects can be obtained up to Mach 0.95 for this type model. Also based on the results shown in references 9 and 10, even though there is a displacement of the terminal shocks at Mach numbers between 0.95 and 0.98 for the larger models, the overall effects on model drag are still small. Larger, more significant effects on drag occur above Mach 0.98. Therefore, it is reasonable to assume that useful data can be obtained with this type model up to Mach 0.98.

As mentioned previously, some small differences were seen in the data between the different size models of the lower Mach numbers. One notable difference appeared near model station $X/L = 0.82$ at the lower speeds. To further investigate the source of these differences an analytical study was made using the potential flow theory (ref. 16). Both the 0.1- and 1.0-percent models were accurately measured at very close intervals and the coordinates input into the program. The resulting calculations of the pressure distribution at Mach 0.9 are shown in figure 13 and compared with the experimental pressures. The results indicate that the experimental differences seen were the result of a very small difference on the model contours between the two configurations.

The effects of model angle of attack on the pressure distribution of the 0.1-percent model at Mach 0.975 are shown in figure 14. Data are presented at angles of attack from 0° to 4° . In general, the effects of increasing angle of attack were to increase the pressure on the underside of the model on the front 70 percent of the model length and to decrease those on top. The pressures over the aft 30 percent of the model were essentially unchanged. Similar results were observed at all Mach numbers.

The effects of removing the model gloves on fuselage pressures with the 0.1-percent model are shown in figure 15 at Mach 0.975 and 0° angle of attack for the pressures along the top of the model. The effects of removing the gloves resulted in a significant change in the pressure distribution in the region of the glove back to about model station $X/L = 0.7$. Little or no effect was observed upstream or downstream of this region. Again similar results were seen at the other Mach numbers.

In figure 16 the effects of the constant chord outboard wing panels on aft fuselage pressures are shown with the 1.0-percent blockage model. Data are presented for the row of pressures along the aft side of the model ($\varphi = 90^\circ$). Model angle-of-attack was zero. Data are presented and compared between the clean wing and the two sizes of constant section wing fairings (fairing at 70-percent semispan and 37-percent semispan, respectively). As can be seen in the data, the effects of the constant section wing panels were negligible up to $M_0 = 0.95$ where a disturbance was generated on the fuselage

between model stations $X/L = 0.65$ and 0.9 . The larger fairing had the larger effect. Increasing Mach number resulted in a larger disturbance. Therefore, it was evident that if a model was used that was supported from its wing tips in this manner a disturbance would be generated at Mach numbers above $M_0 = 0.95$.

Several attempts were made to minimize the adverse effects of the constant section wings. These included variations in local tunnel porosity and variations in tunnel sidewall geometry. When tunnel porosity was varied, the only change that generated positive results was the sidewall porosity conditions near the wing tip. The effects of varying tunnel sidewall porosity near the wing tips are shown in figure 17. Changes in tunnel porosity were done only with the large wing fairings present. When the tunnel sidewall porosity was changed from 3.1 percent (half) open to 6.1 percent (full) open (note the porosity difference seen in the photographs shown in figs. 4(d) and 6(b)), the adverse effects on the pressures were reduced up to Mach 0.975. At the higher Mach numbers the change in porosity was not sufficient to eliminate the disturbance. Also further increases in porosity upstream and downstream of this region had no effect.

The effects of the contoured sidewall with the large wing fairings are shown in figure 18. As stated previously, the contoured sidewall was an attempt to minimize the adverse effects of the wing fairing by opening up the tunnel flow area to account for the added blockage. As seen in figure 18 the results were to generate a new disturbance on the aft fuselage pressures which became apparent for Mach numbers above $M_0 = 0.95$. The results of this attempt do not mean, however, that this approach could not be used successfully but instead, that more work is required.

The effects of a simulated forward swept support strut on aft fuselage pressures are shown in figure 19. Data are presented at Mach 0.975 and a 0° angle of attack for the pressures on the bottom side of the model. This test was conducted with the large wing fairings in place but with the 6.1-percent porosity at the wing tips. As can be seen in figure 19 the effect of the strut on aft fuselage pressures was negligible. However, small effects were seen on the fuselage pressures near the strut fuselage intersection. Similar results were seen at all other Mach numbers. No attempt was made to determine the effect of the strut on the downstream boundary layer or total pressures near the model.

SUMMARY OF RESULTS

To investigate the effects of model blockage and support interference with winged-body configurations, a series of tests were conducted in the Lewis Research Center's 8- by 6-Foot Supersonic Wind Tunnel with several sizes of calibration models. Fuselage pressures were measured for three sting-mounted models, which included ratios of

maximum model cross-sectional area to test-section area (blockage) of 0.1, 1.0, and 2.0 percent. Two other types of model support were investigated with the 1.0-percent blockage model. These included simulated wing-tip and fuselage support-strut type mountings. The effects of altering local tunnel porosity and tunnel sidewall geometry were also investigated. A 0.1-percent blockage axisymmetric model was also tested for reference. Data were obtained over a Mach number range of 0.6 to 1.0 at angles of attack from 0° to 4° .

The following observations were made:

1. Axisymmetric 0.1-percent blockage model data indicate no significant disturbances up to Mach 0.975. Above Mach 0.975 a disturbance probably resulting from both the presence of the model sting and a displacement of the transonic terminal shock is present on the aft region of the model. Good agreement with data from a 0.2-percent blockage model tested in another facility was also observed. And good agreement with predictions from local linearization theory was obtained except where there were regions of supercritical flow.

2. Tunnel blockage effects on the fuselage pressures of the winged-body configurations were generally small for Mach numbers less than 0.95. At Mach 0.95 and above displacements of two separate transonic terminal shocks were observed for the higher blockage models. Two terminal shocks resulted because of the area-ruled geometry of the fuselage. The first shock was displaced upstream with increasing blockage, and the second was displaced further aft. The most significant displacement was generally seen between the 0.1- and 1.0-percent blockage models. An increase in blockage from 1.0 to 2.0 percent resulted, therefore, in only a small additional displacement of these shocks.

3. Some of the observed differences in the data comparisons between the various size models was attributable to small local differences in the model surface contours.

4. The effect of increasing angle of attack was to alter the pressures forward on the model but had little effect on the pressures aft on the model. The pressures on the lower surface of the forward fuselage generally increased with increasing angle of attack while those on the upper surface decreased.

5. Alterations in the model cross-sectional area distribution by removing the wing gloves resulted in relatively local changes of the fuselage pressures.

6. The effect of a simulated wing-tip model support (by using a constant section panel from a given semispan position to the tunnel wall) was to generate a disturbance on the aft region of the fuselage at Mach numbers from 0.95 to 1.0. Increasing Mach number resulted in an increased magnitude of the disturbance. Local changes in tunnel porosity, however, reduced this disturbance up to $M_0 = 0.975$.

7. The effects of a lower fuselage forward swept strut were generally small near the strut-model intersection and negligible over the rest of the model.

Lewis Research Center,
National Aeronautics and Space Administration,
Cleveland, Ohio, September 5, 1973,
501-24.

REFERENCES

1. Langhans, Richard A. ; and Flechner, Stuart G. : Wind Tunnel Investigation at Mach Numbers From 0.25 to 1.01 of a Transport Configuration Designed to Cruise at Near Sonic Speeds. NASA TM X-2622, 1972.
2. Braslow, Albert L. ; and Alford, William J. : Advanced Subsonic Transport Technology Assessment; Overview: Keeping Air Leadership. Astronautics and Aeronautics, vol. 10, no. 8, Aug. 1972, pp. 27-31.
3. Ayers, Theodore G. : Advanced Subsonic Transport Technology Assessment; Supercritical Aerodynamics: Worthwhile Over a Range of Speeds. Astronautics and Aeronautics, vol. 10, no. 8, Aug. 1972, pp. 32-36.
4. Beheim, Milton A. ; Antl, Robert J. ; and Povolny, John H. : Advanced Subsonic Transport Technology Assessment; Advanced Propulsion: Cleaner and Quieter. Astronautics and Aeronautics, vol. 10, no. 8, Aug. 1972, pp. 37-43.
5. Schwartz, M. B. : Propulsion System Requirements for Advanced Technology Air Transports. Paper 710761, SAE, Sept. 1971.
6. Goodmanson, Lloyd T. ; and Schultz, William H. : Installation and Integration of Transonic Transport Propulsion Systems. Paper 710762, SAE, Sept. 1971.
7. Black, Richard E. ; Murphy, David G. ; and Stern, John A. : The Crystal Ball Focuses on the Next Generation of Transport Aircraft. Paper 710750, SAE, Sept. 1971.
8. Sussman, M. B. ; Gunnarson, D. W. ; and Edwards, P. : Nacelle Design Studies for Advanced Transport Aircraft. Paper 72-1204, AIAA, Nov.-Dec. 1972.
9. Couch, Lana M. : Transonic Wall Interference Effects on Bodies of Revolution. Paper 72-1008, AIAA, Sept. 1972.

10. Couch, Lana M.; and Brooks, Cuyler W., Jr.: Effect of Blockage Ratio on Drag and Pressure Distributions for Bodies of Revolution at Transonic Speeds. NASA TN D -7331, 1973.
11. Mitchell, Glenn A.: Blockage Effects of Cone-Cylinder Bodies on Perforated Wind Tunnel Wall Interference. NASA TM X-1655, 1968.
12. Mitchell, Glenn A.: Effect of Model Forebody Shape on Perforated Tunnel Wall Interference. NASA TM X-1656, 1968.
13. Blaha, Bernard J.; and Bresnahan, Donald L.: Wind Tunnel Installation Effects on Isolated Afterbodies at Mach Numbers From 0.56 to 1.5. NASA TM X-52581, 1969.
14. Taylor, Robert A.; and McDevitt, John B.: Pressure Distributions at Transonic Speeds for Parabolic-Arc Bodies of Revolution Having Fineness Ratios of 10, 12, and 14. NACA TN 4234, 1958.
15. Spreiter, John R.; and Alksne, Alberta Y.: Slender-Body Theory Based on Approximate Solution of the Transonic Flow Equation. NASA TR-2, 1959.
16. Hess, J. L.; and Smith, A. M. O.: Calculation of Potential Flow About Arbitrary Bodies. In Progress in Aeronautical Sciences. Vol. 8, D. Kuchewann, ed., Pergamon Press, Ltd., 1967, pp. 1-138.

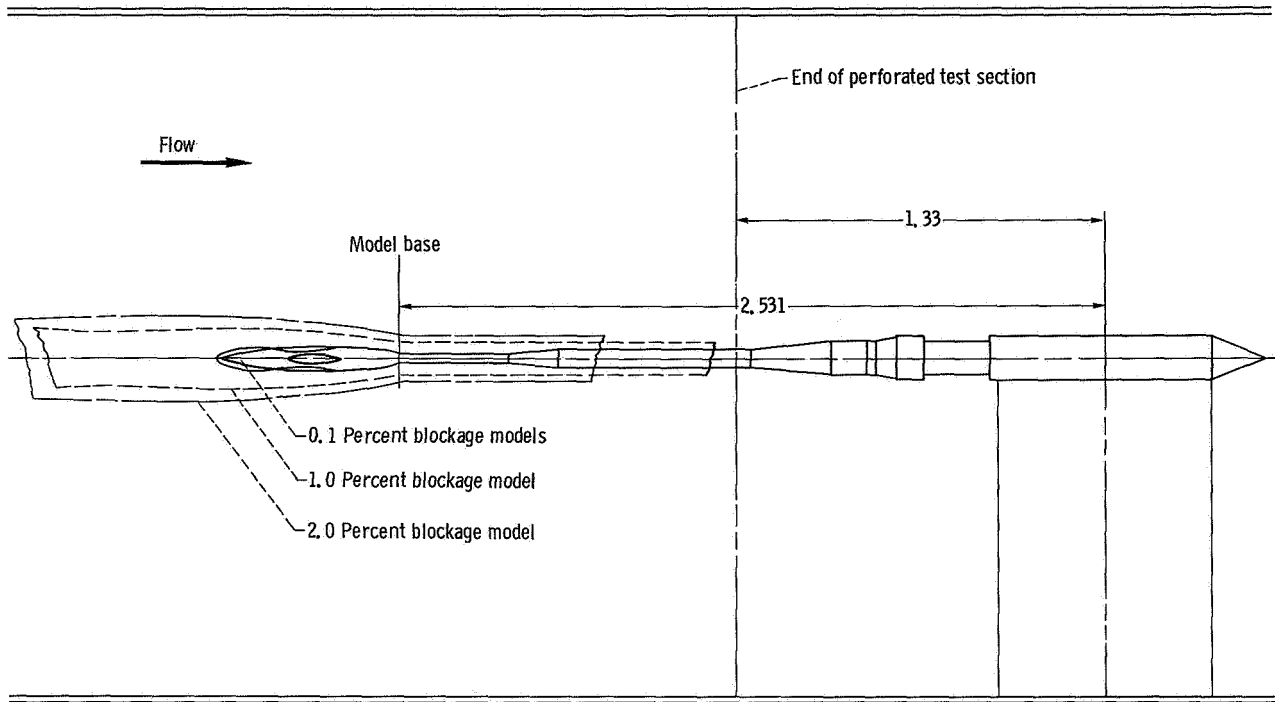
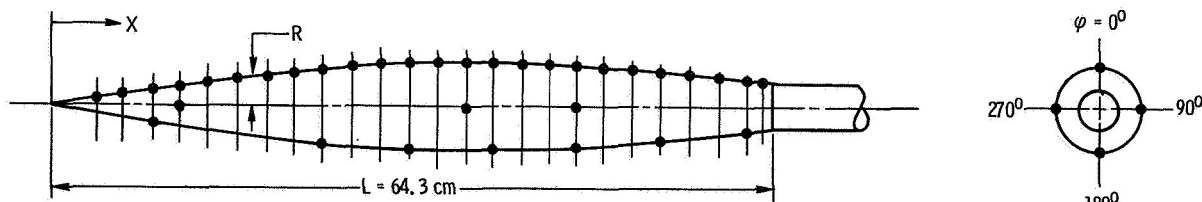


Figure 1. - Schematic of model installation in transonic test section of 8- by 6-foot Supersonic Wind Tunnel. (Dimensions are in m.)



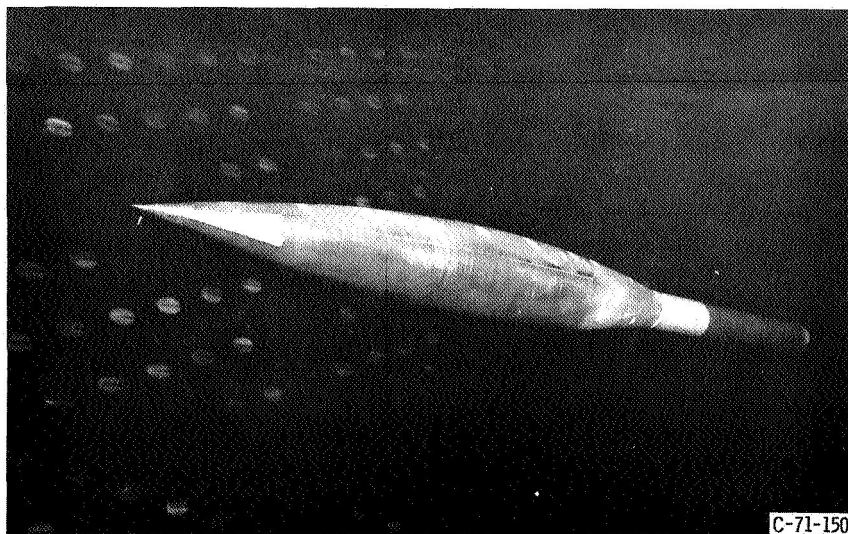
Coordinates

X/L	R/L
0.035	0.007
.070	.013
.105	.019
.152	.027
.187	.032
.223	.036
.269	.042
.304	.045
.339	.048
.386	.052
.421	.054
.468	.056
.504	.057
.538	.058
.574	.059
.620	.0583
.656	.058
.691	.057
.738	.055
.773	.053
.820	.049
.855	.046
.890	.043
.936	.038
.972	.033
1.000	.029

Pressure orifice locations

X/L	Angular position coordinate, ϕ , deg
0.051	0
.083	0, 90
.119	0, 180
.153	0, 90, 270
.187	0
.221	0, 90, 180
.255	0
.288	0, 90
.322	0, 180
.356	0, 90
.390	0
.424	0, 90, 180
.459	0
.492	0, 90, 270
.526	0, 180
.561	0, 90
.595	0
.628	0, 90, 180, 270
.660	0
.695	0, 90
.729	0, 180
.764	0, 90
.797	0
.832	0, 90, 180
.849	0

(a) Model dimensions.



(b) Photograph of model in wind tunnel.

Figure 2. - Details of axisymmetric, parabolic-arc, 0.1 percent blockage.

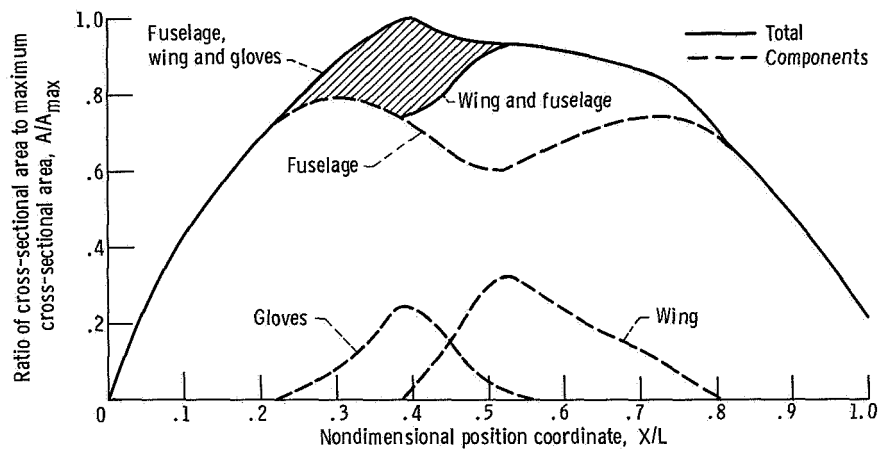
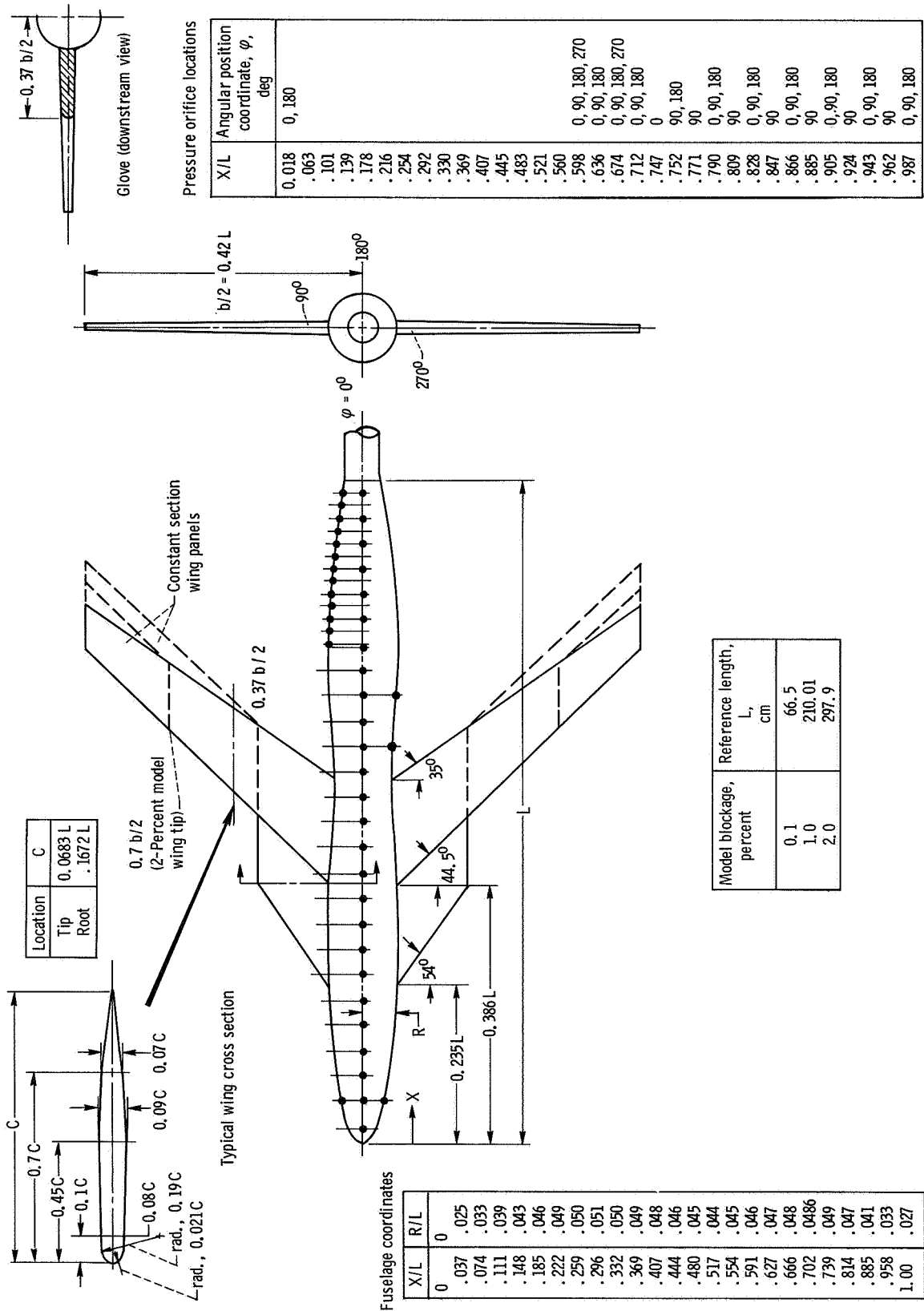
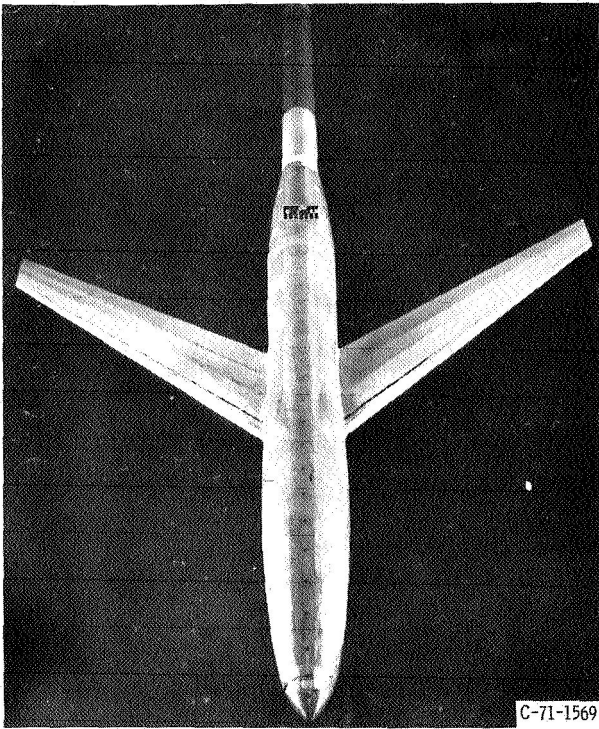


Figure 3. - Cross-sectional area distribution of winged-body models.

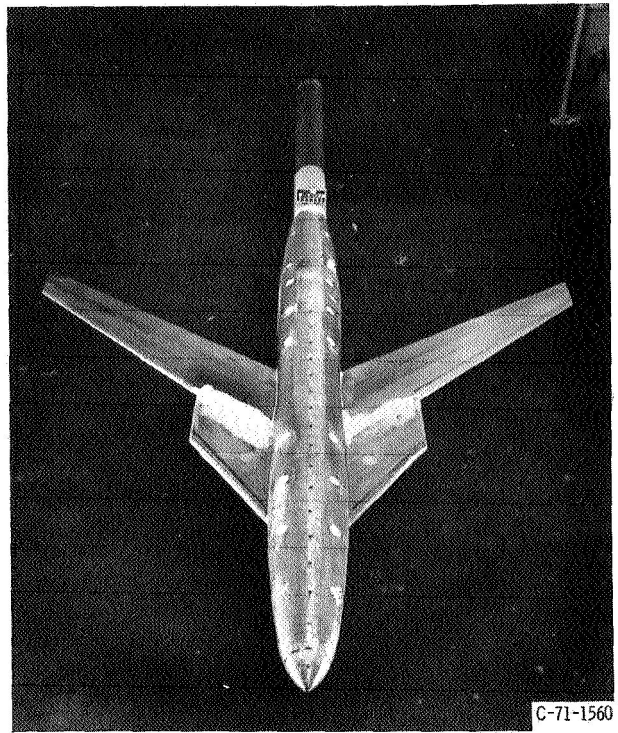


(a) Model dimensions.

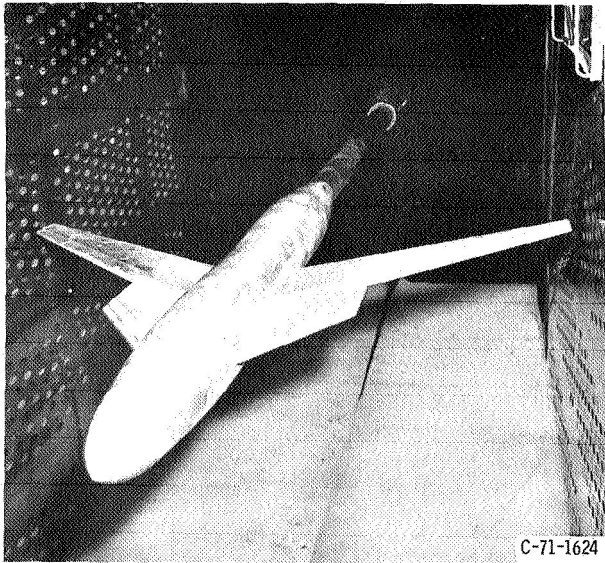
Figure 4. - Details of winged-body configurations.



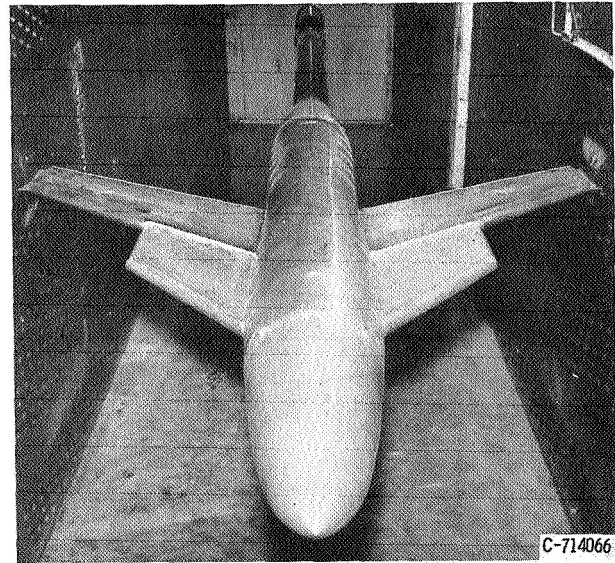
(b) 0.1-Percent blockage model in wind tunnel without gloves.



(c) 0.1-Percent blockage model in wind tunnel with gloves.



(d) 1.0-Percent blockage model in wind tunnel.



(e) 2-Percent blockage model in wind tunnel.

Figure 4. - Concluded.

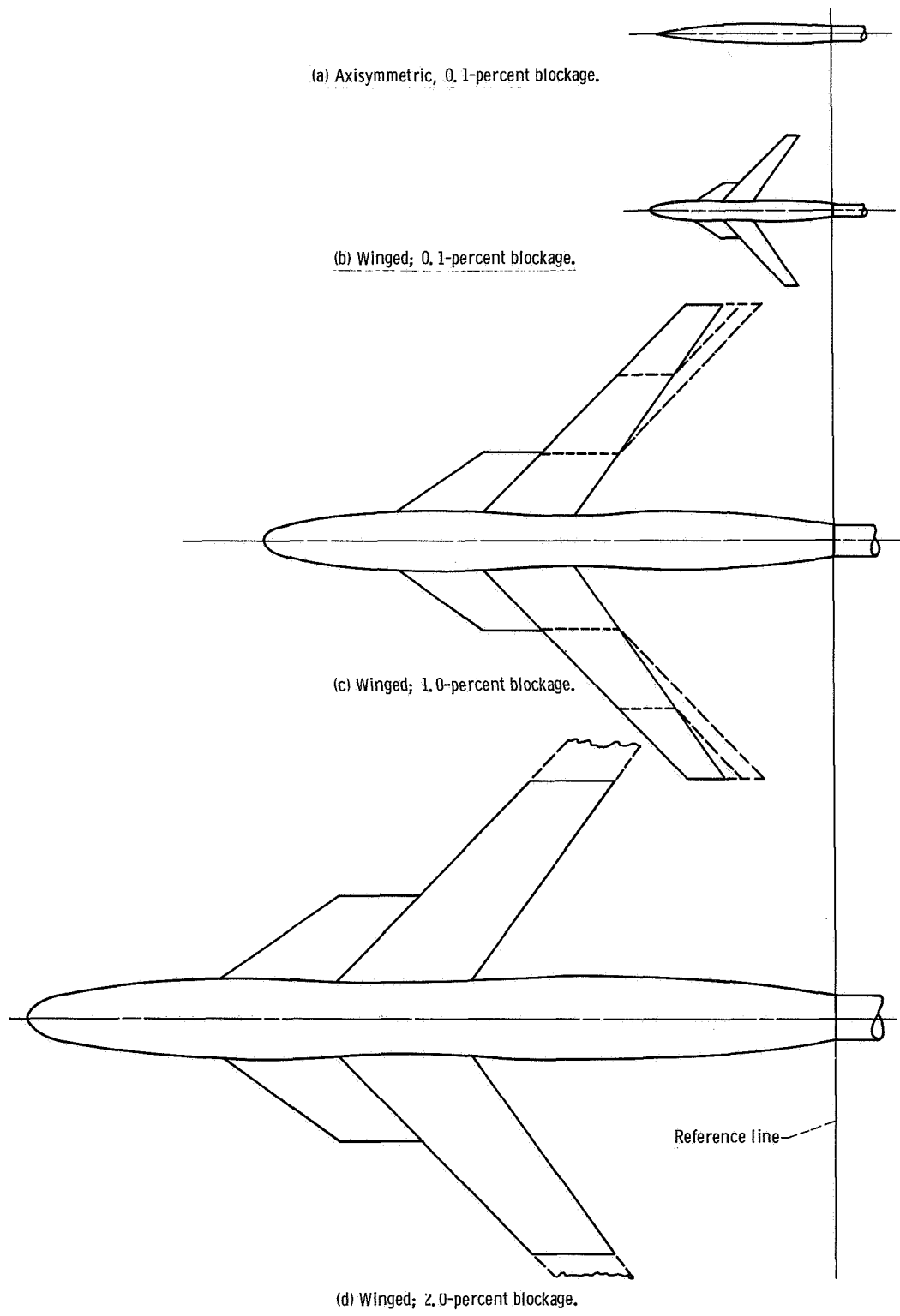
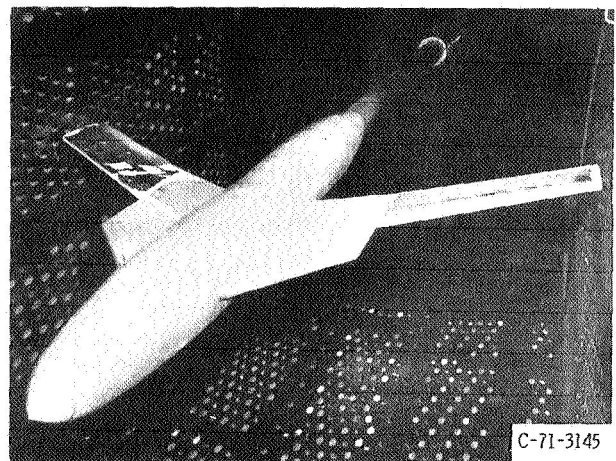


Figure 5. - Comparison of blockage model relative sizes.

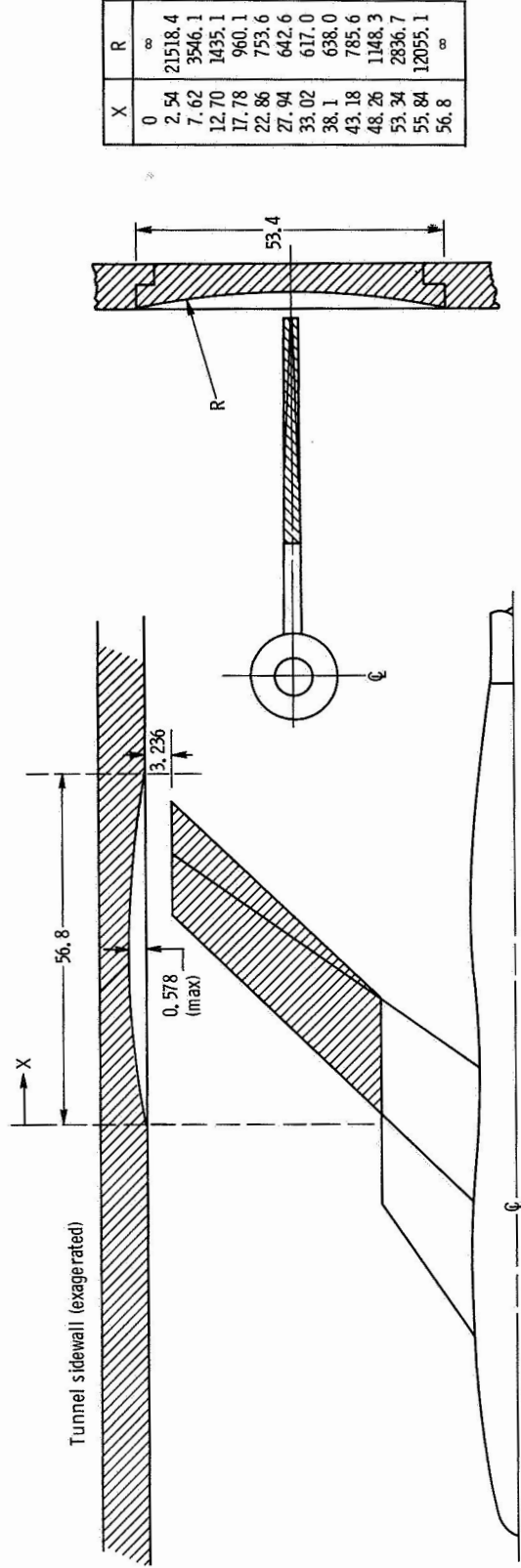


(a) Wing section constant at 0.7 semispan.



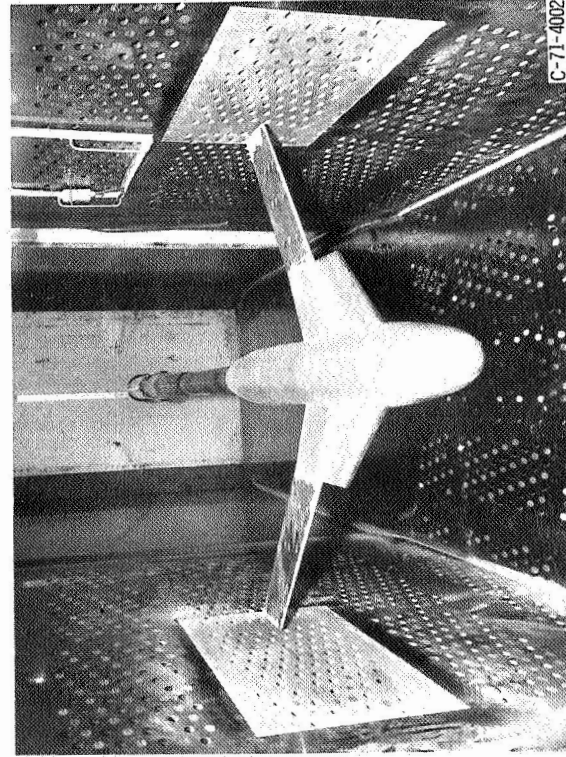
(b) Wing section constant at 0.37 semispan.

Figure 6. - 1.0-Percent blockage model with simulated constant section wing panels.

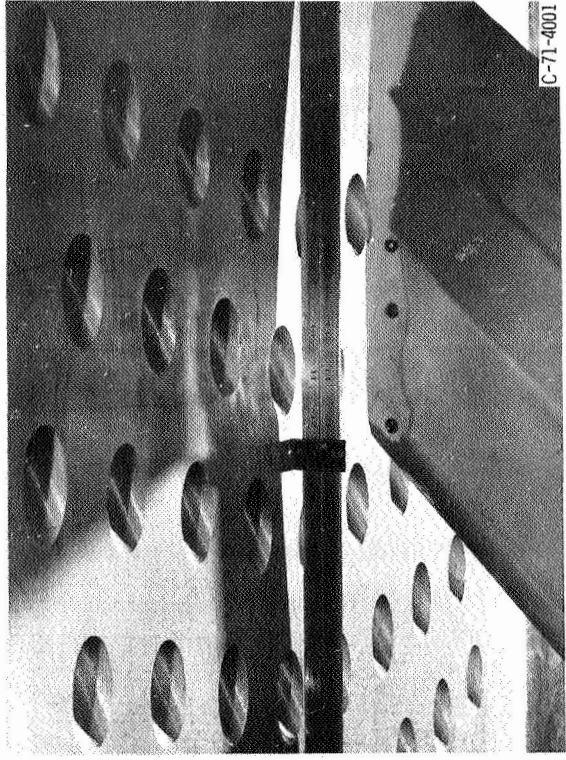


(a) Top view.

(b) Upstream view.

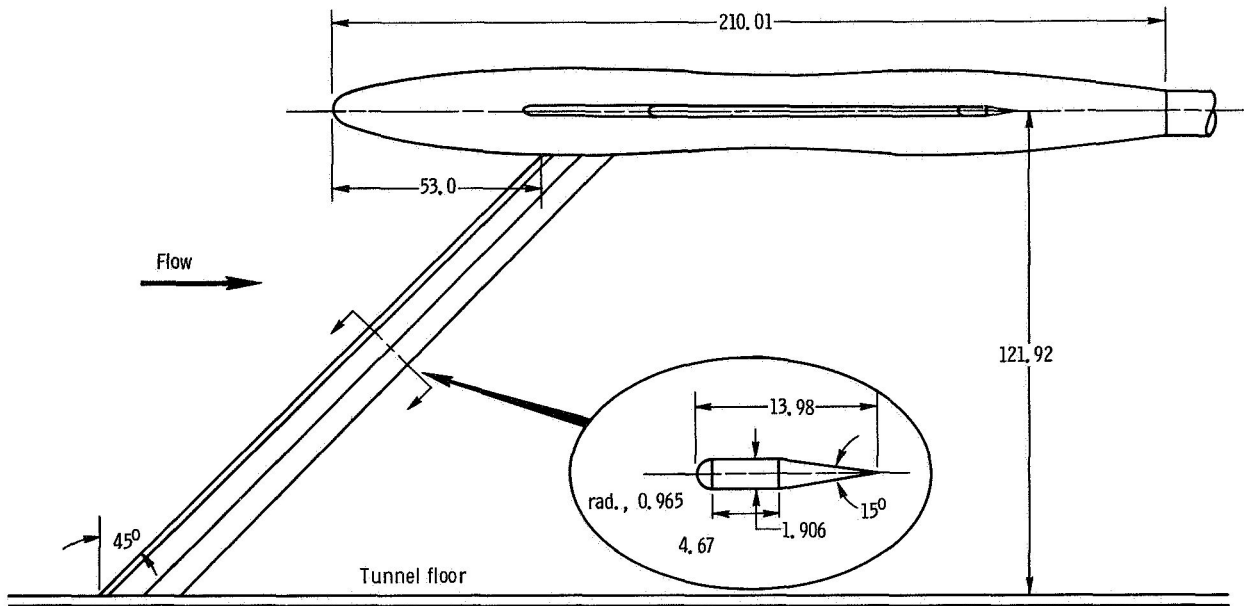


(c) Model installed in tunnel.

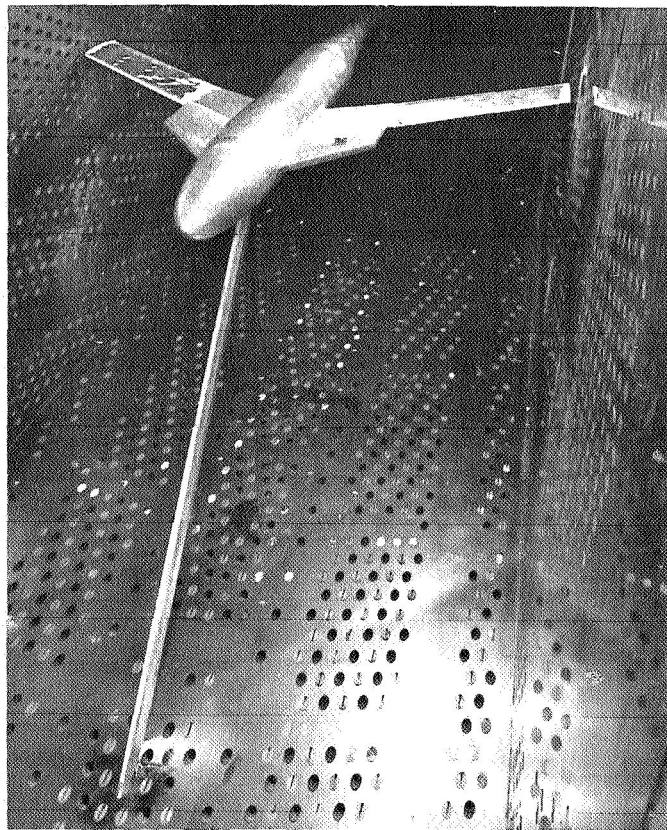


(d) Close-up showing wall contour.

Figure 7. - Details of tunnel sidewall modification used with 1.0-percent blockage models. (Dimensions are in cm.)



(a) Strut dimensions.



(b) Photograph showing installation in tunnel.

Figure 8. - Details of simulated swept strut on 1.0-percent blockage model. (Dimensions are in cm.)

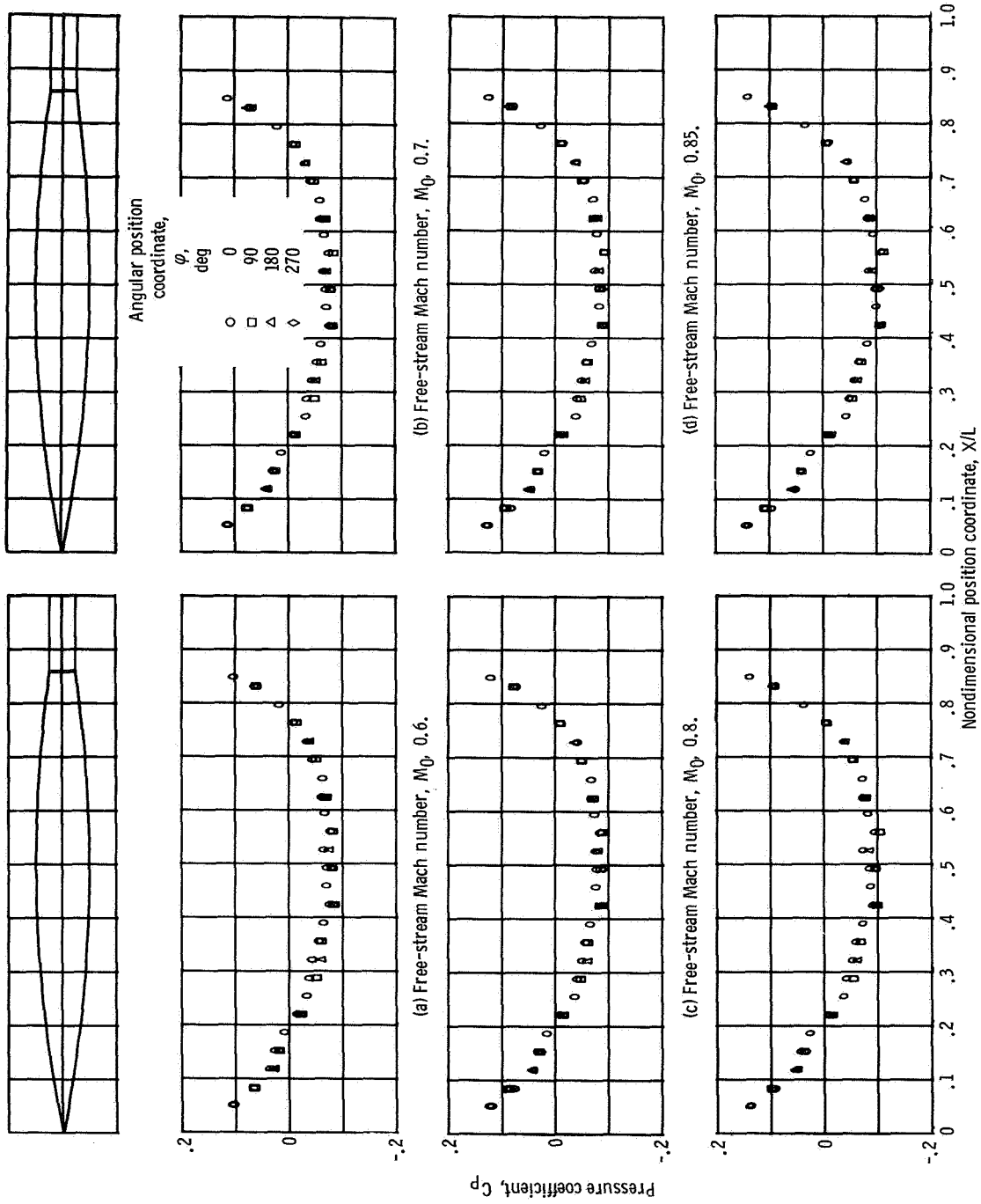


Figure 9. - Axisymmetric 0.1-percent model pressure distributions. Angle of attack, α , 0° .

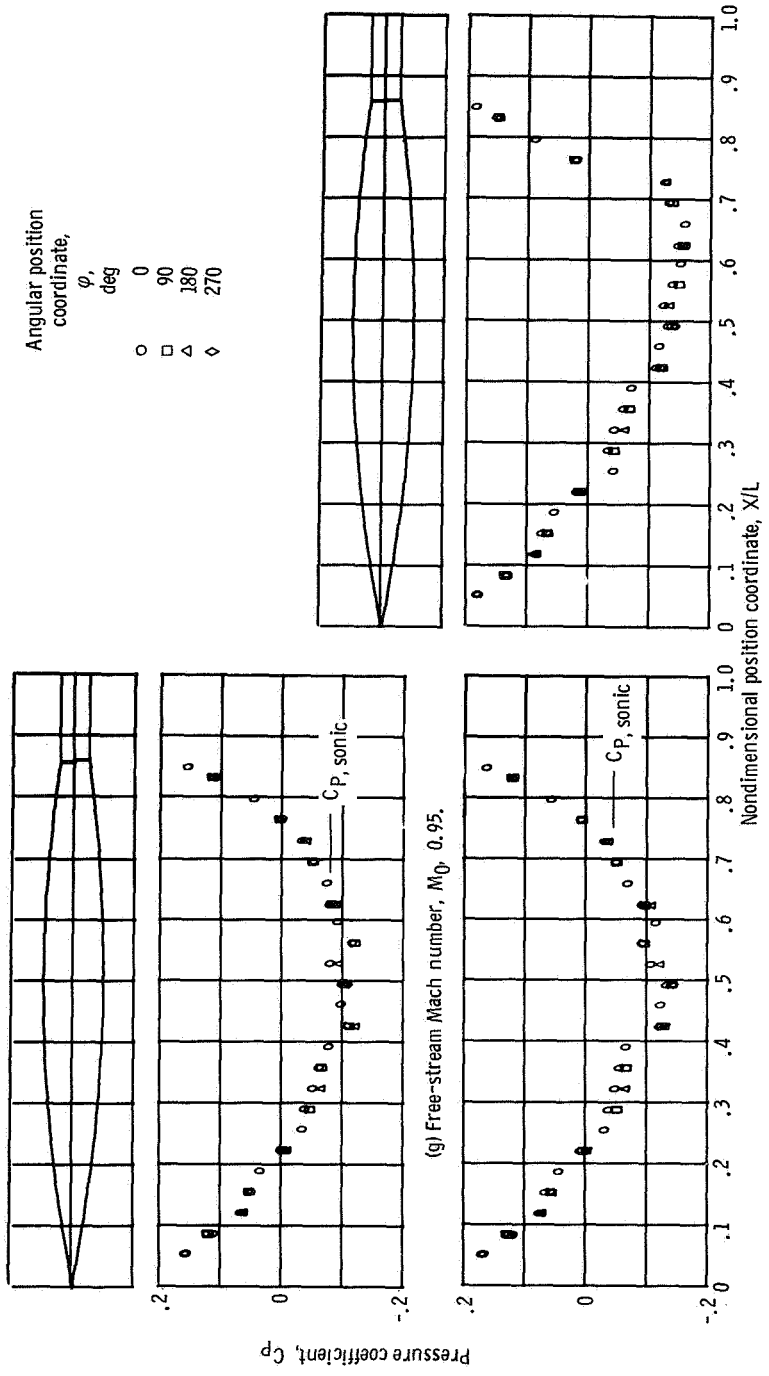


Figure 9. - Concluded.

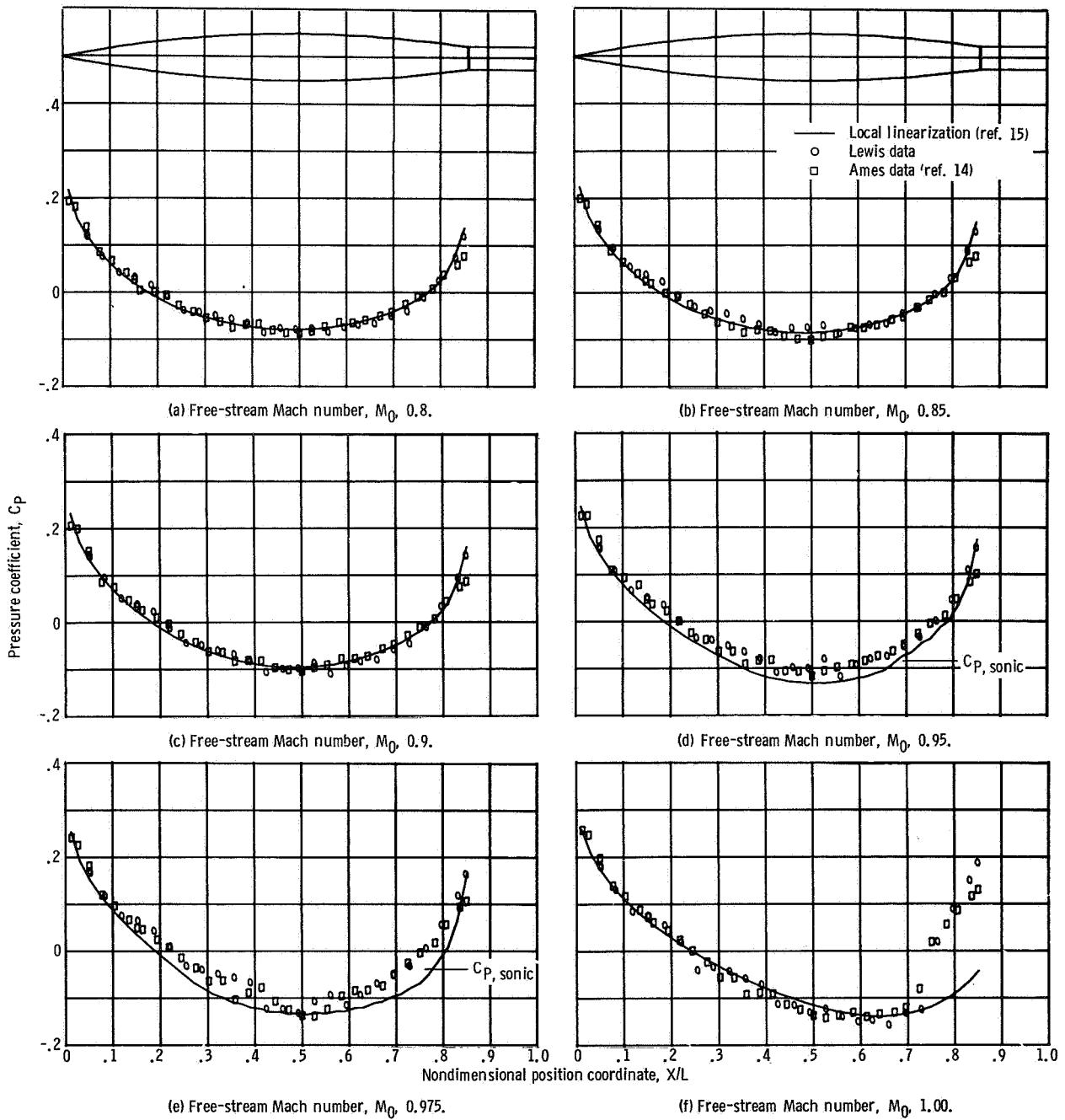
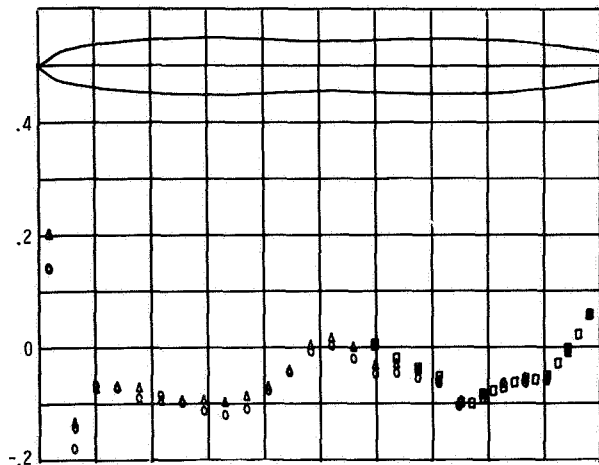
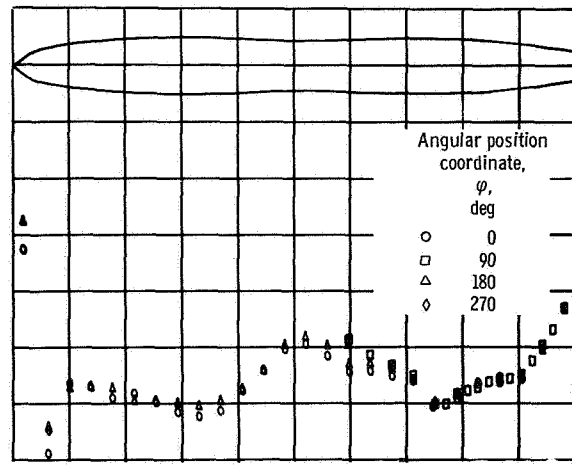


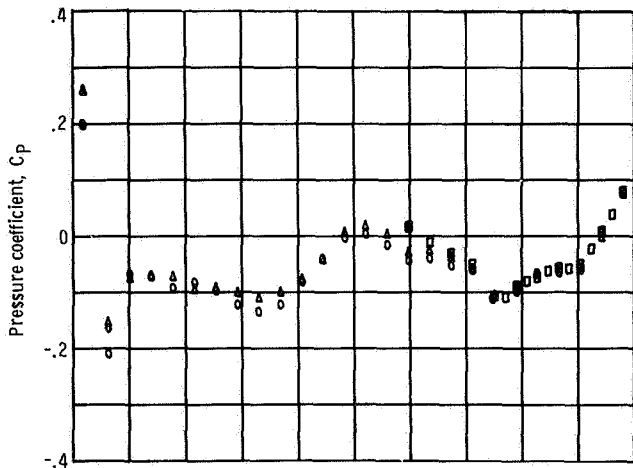
Figure 10. - Comparison of axisymmetric 0.1-percent blockage model pressure distributions with theoretical predictions and data from a 0.2-percent blockage model tested in another facility.



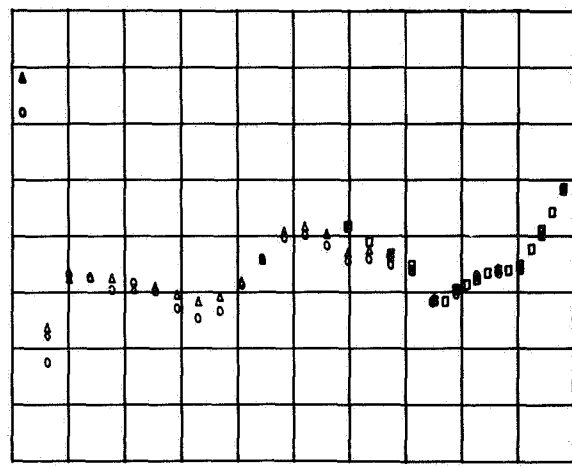
(a) Free-stream Mach number, M_0 , 0.6.



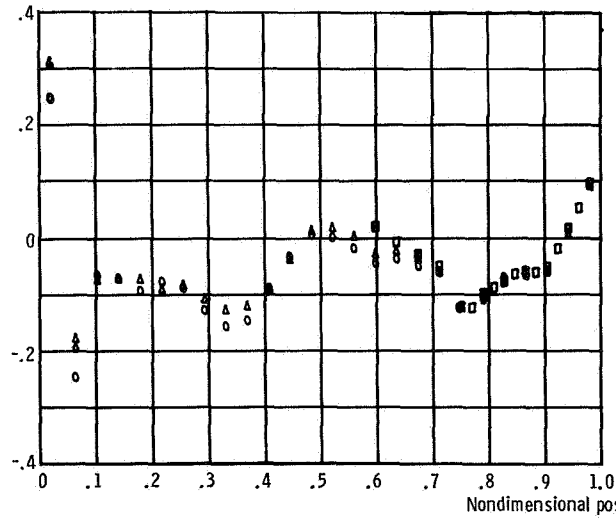
(b) Free-stream Mach number, M_0 , 0.7.



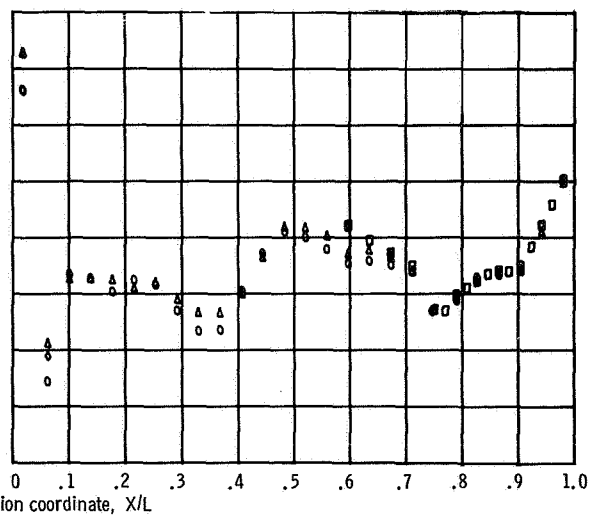
(c) Free-stream Mach number, M_0 , 0.8.



(d) Free-stream Mach number, M_0 , 0.85.



(e) Free-stream Mach number, M_0 , 0.9.



(f) Free-stream Mach number, M_0 , 0.925.

Figure 11. - Winged body pressure distributions, 0, 1-percent blockage model at 0° angle of attack.

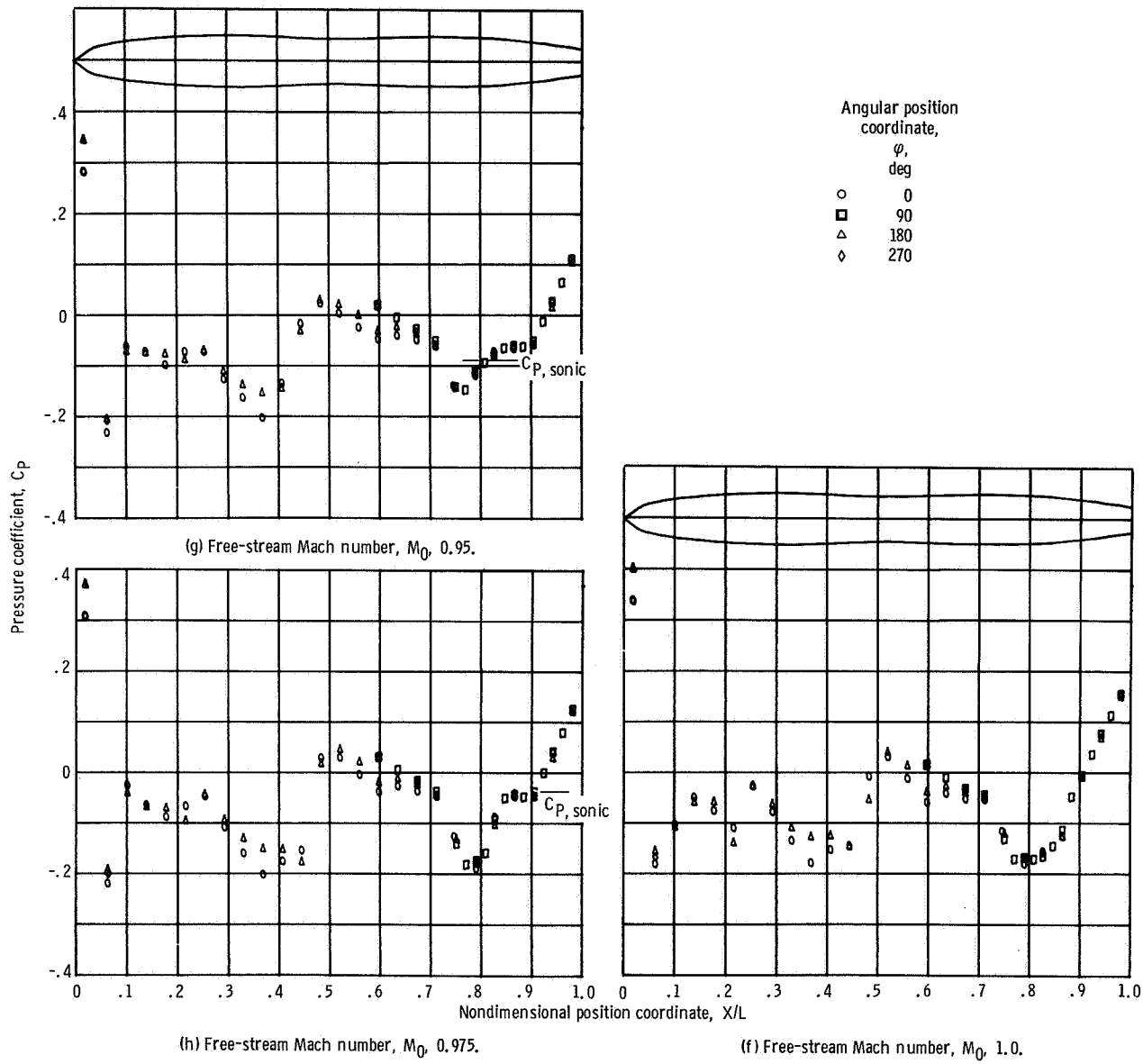


Figure 11. - Concluded.

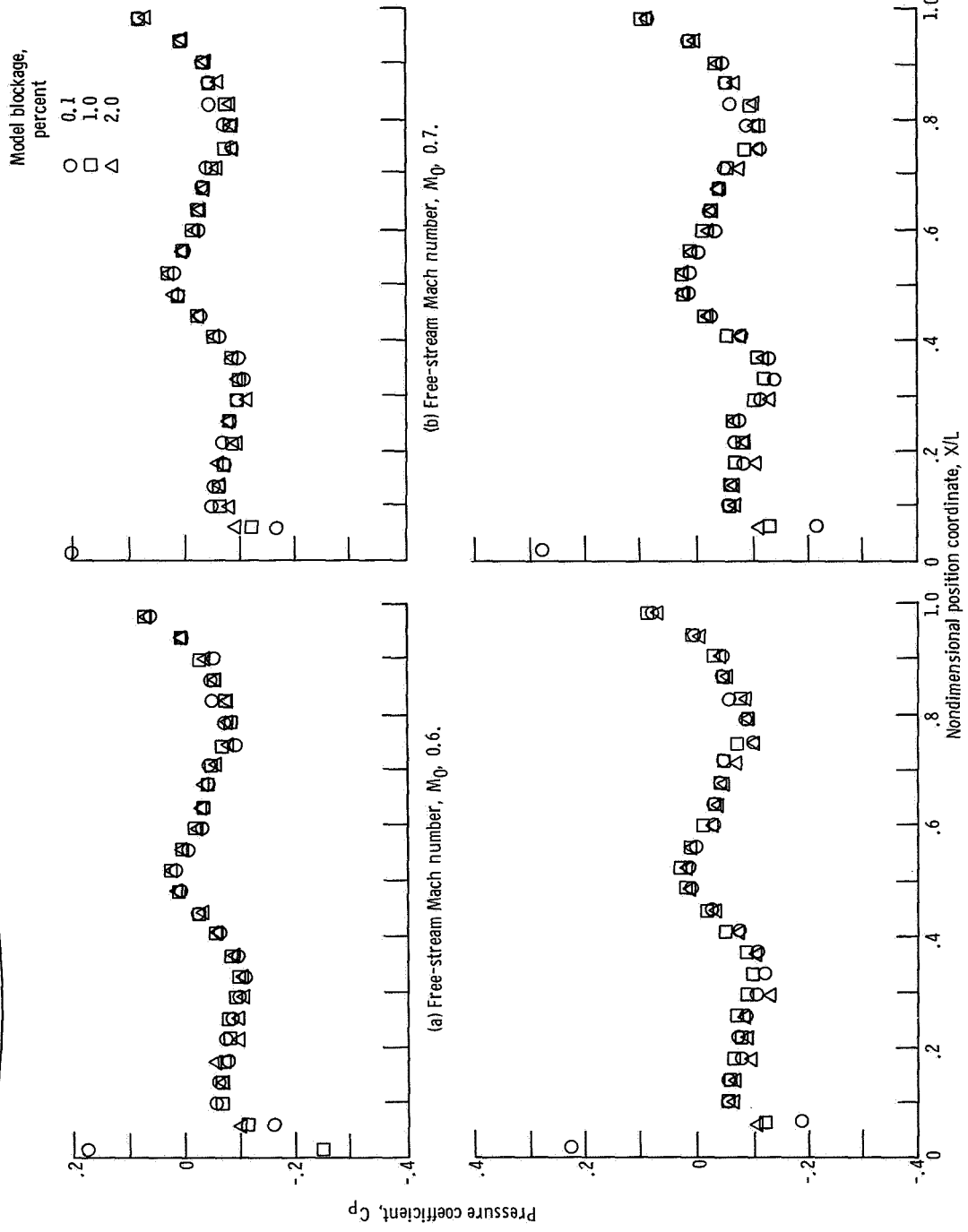
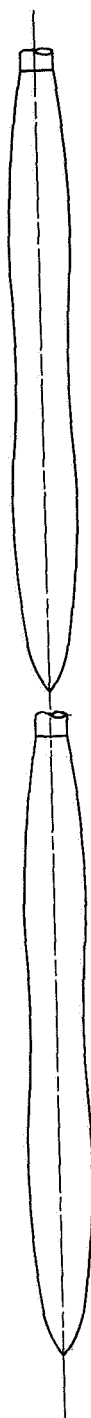


Figure 12. - Effect of model blockage on fuselage pressure distribution. Angular position coordinate, φ , 0° ; angle of attack, α , 0° .

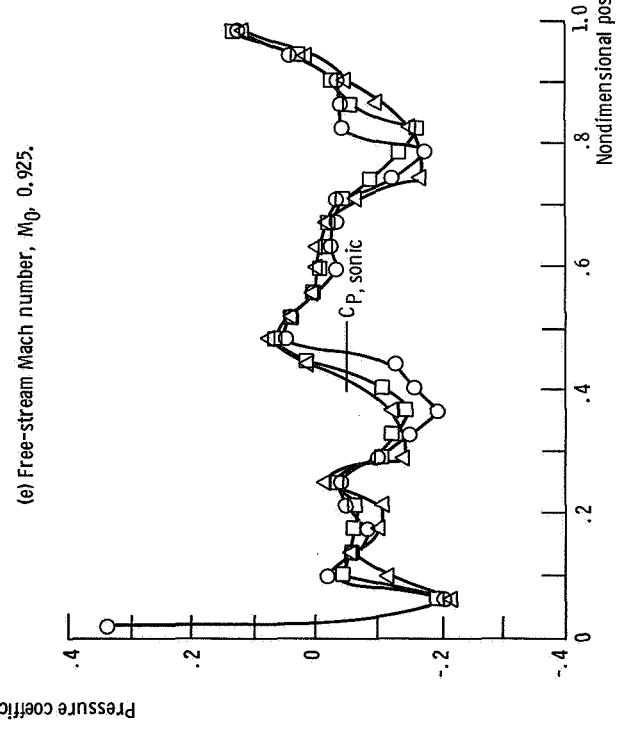
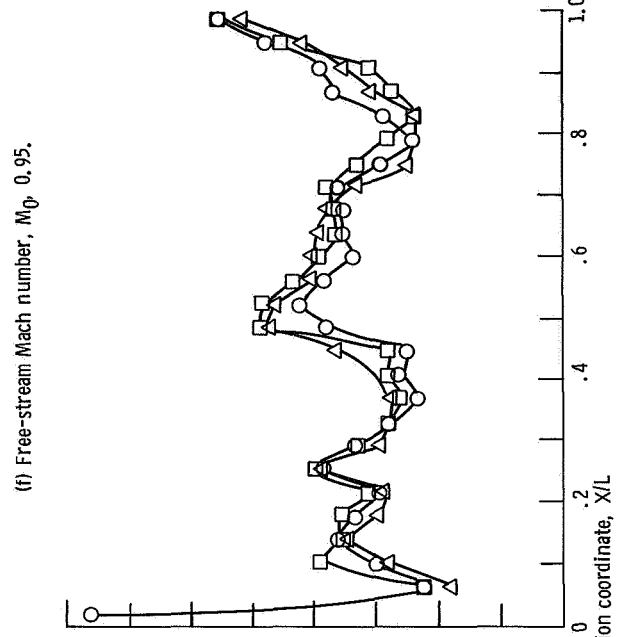
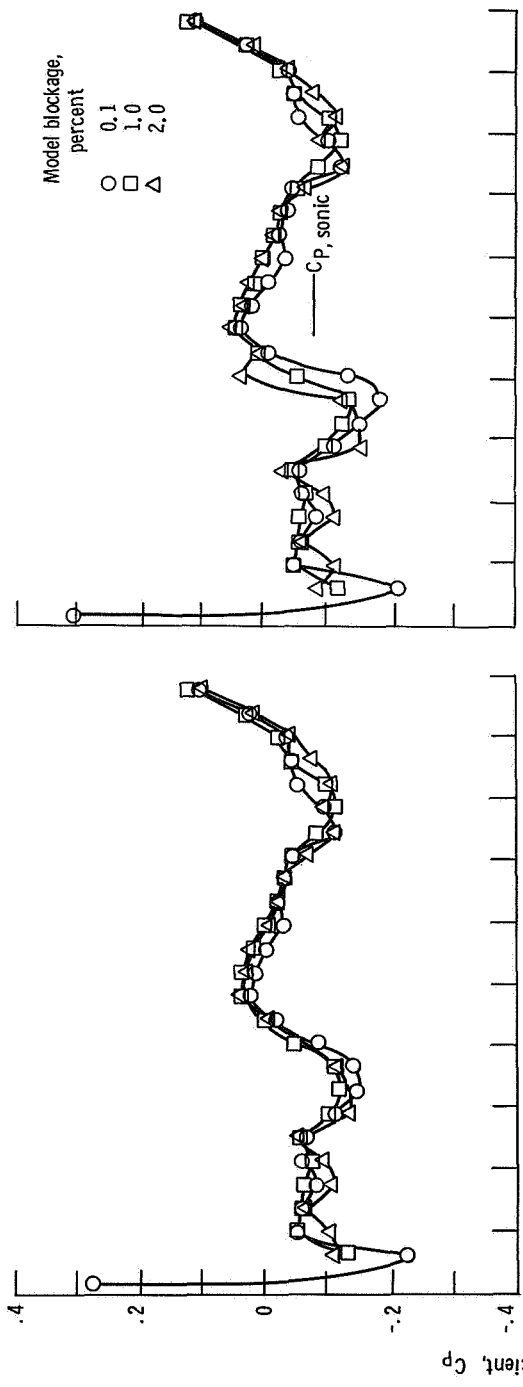
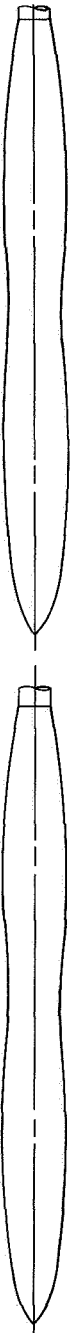


Figure 12. - Concluded.

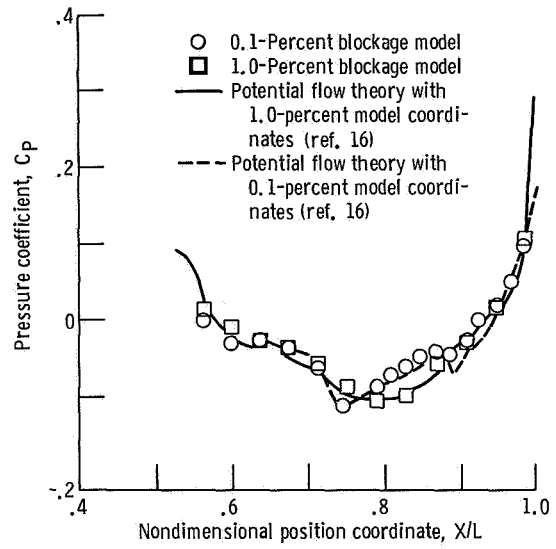


Figure 13. - Effect of model surface variances on pressure distribution. Free-stream Mach number, M_0 , 0.9; angle of attack, α , 0° ; model angular coordinate, φ , 90° .

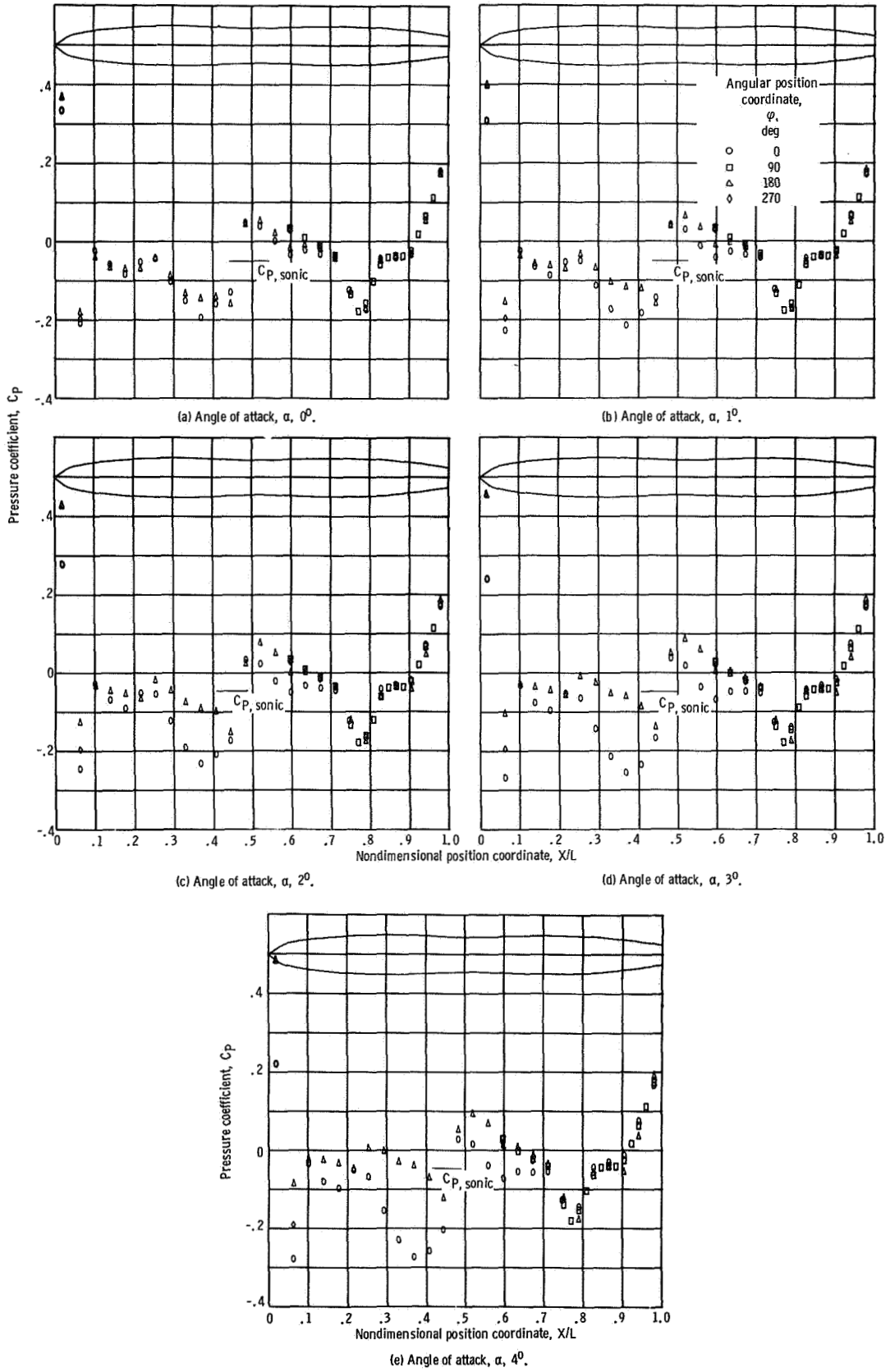


Figure 14. - Effect of model angle of attack on 0.1-percent blockage model pressure distribution at free-stream Mach number, $M_0, 0.975$.

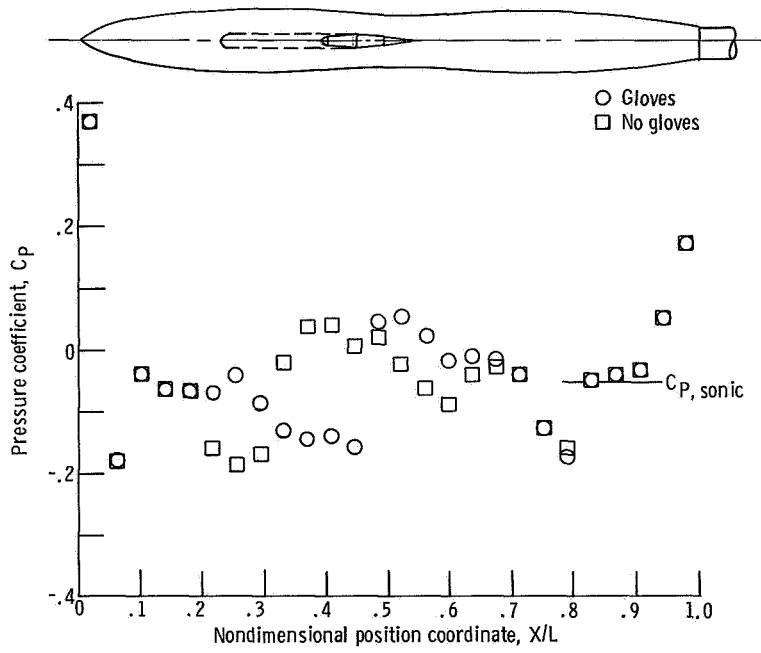


Figure 15. - Effect of removal of simulated wing glove on pressure distribution of 0.1-percent blockage model. Free-stream Mach number, M_0 , 0.975; angle of attack, α , 0° ; angular position coordinate, φ , 0° .

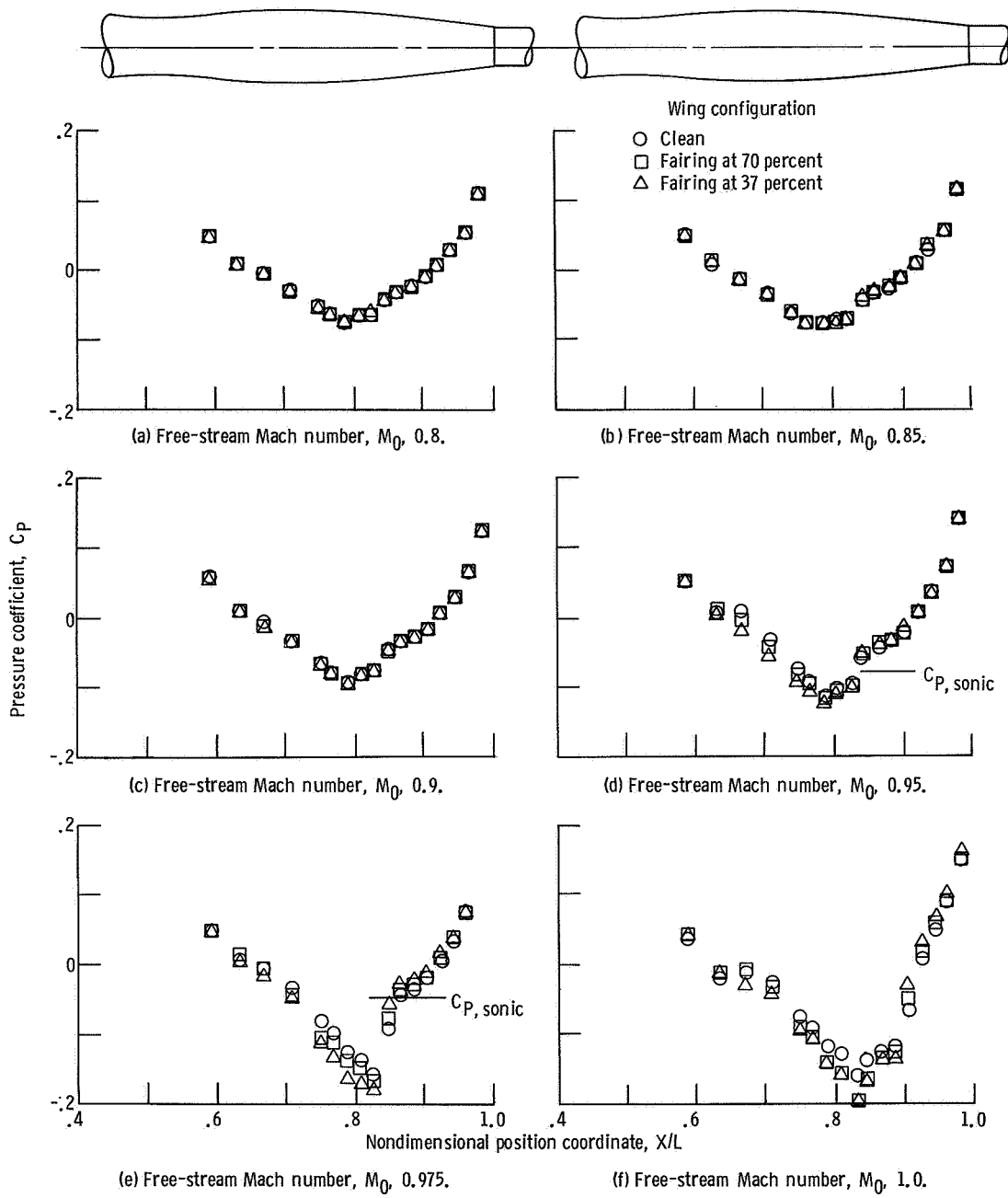


Figure 16. - Effect of constant chord outboard wing panel on fuselage pressures with the 1-percent blockage model. Angular position coordinate, φ , 90° ; angle of attack, α , 0° .

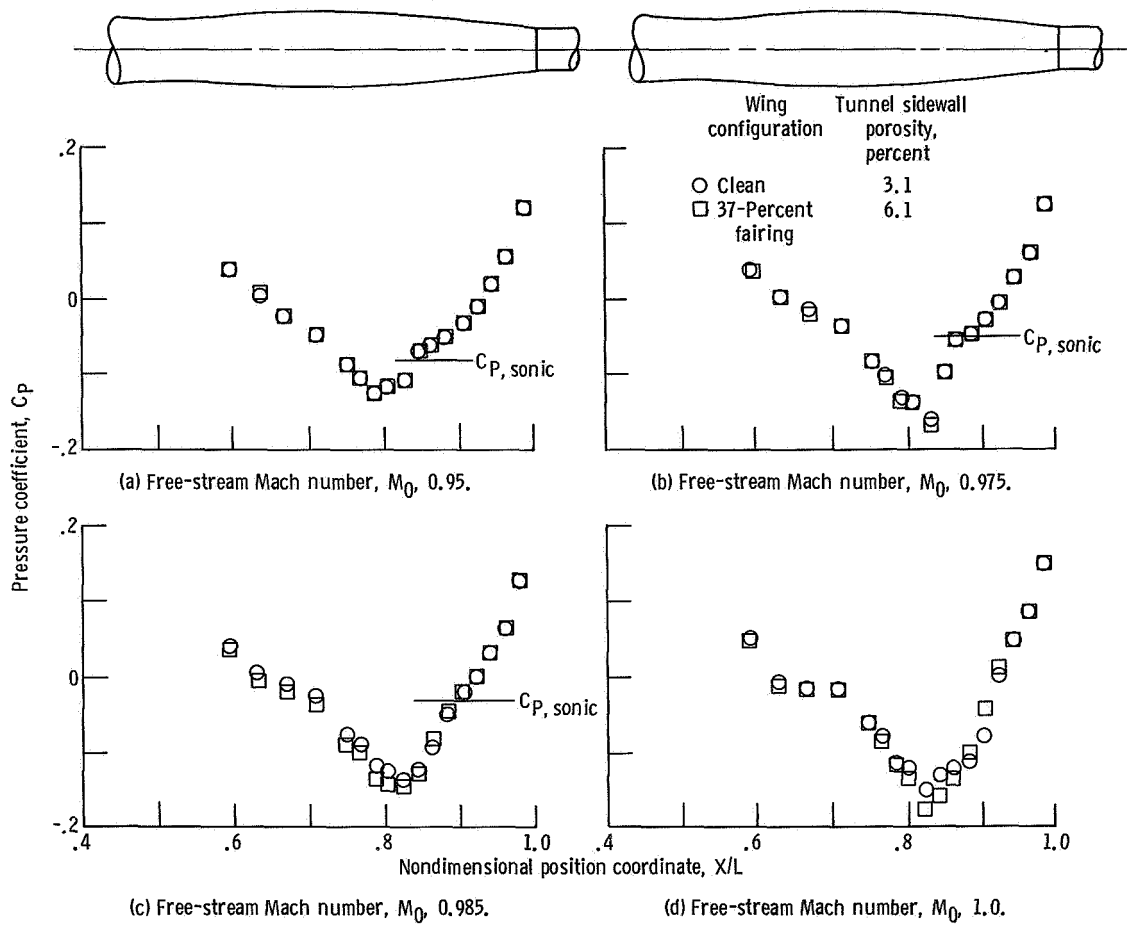


Figure 17. - Effect of increased tunnel sidewall porosity at wing tip for 1-percent blockage model. Angular position coordinate, φ , 90° ; angle of attack, α , 0° .

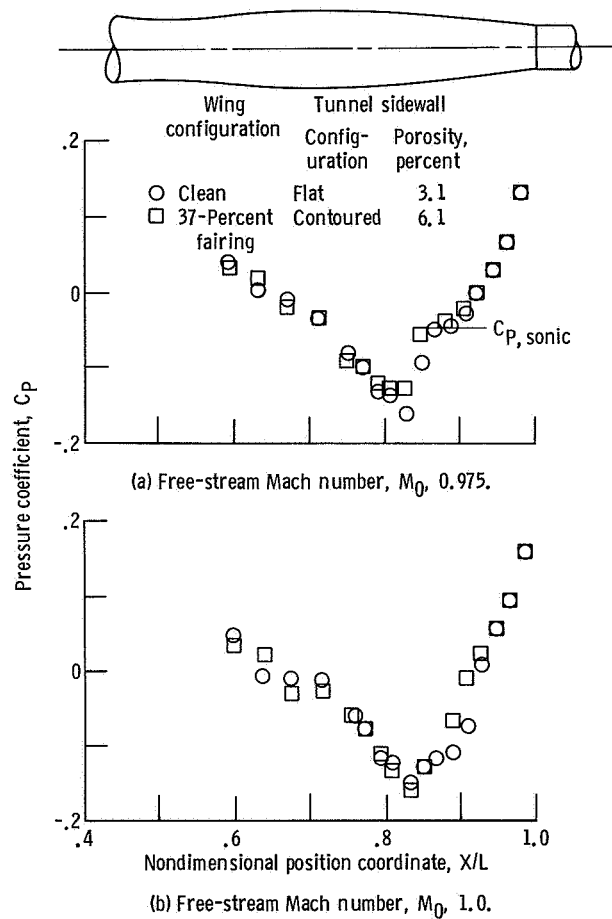


Figure 18. - Effect of contoured tunnel sideplates on fuselage pressures of 1-percent blockage model. Angular coordinate, φ , 90° ; angle of attack, α , 0° .

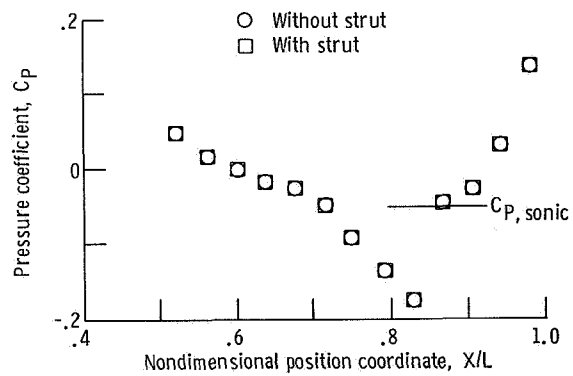


Figure 19. - Effect of forward support strut on aft fuselage pressure distribution of 1.0-percent blockage model. Free-stream Mach number, M_0 , 0.975; angular coordinate position, φ , 180° ; angle of attack, α , 0° .

NATIONAL AERONAUTICS AND SPACE ADMINISTRATION
WASHINGTON, D.C. 20546

OFFICIAL BUSINESS
PENALTY FOR PRIVATE USE \$300

**SPECIAL FOURTH-CLASS RATE
BOOK**

POSTAGE AND FEES PAID
NATIONAL AERONAUTICS AND
SPACE ADMINISTRATION
451



POSTMASTER: If Undeliverable (Section 108
Postal Manual) Do Not Return

"The aeronautical and space activities of the United States shall be conducted so as to contribute . . . to the expansion of human knowledge of phenomena in the atmosphere and space. The Administration shall provide for the widest practicable and appropriate dissemination of information concerning its activities and the results thereof."

—NATIONAL AERONAUTICS AND SPACE ACT OF 1958

NASA SCIENTIFIC AND TECHNICAL PUBLICATIONS

TECHNICAL REPORTS: Scientific and technical information considered important, complete, and a lasting contribution to existing knowledge.

TECHNICAL NOTES: Information less broad in scope but nevertheless of importance as a contribution to existing knowledge.

TECHNICAL MEMORANDUMS: Information receiving limited distribution because of preliminary data, security classification, or other reasons. Also includes conference proceedings with either limited or unlimited distribution.

CONTRACTOR REPORTS: Scientific and technical information generated under a NASA contract or grant and considered an important contribution to existing knowledge.

TECHNICAL TRANSLATIONS: Information published in a foreign language considered to merit NASA distribution in English.

SPECIAL PUBLICATIONS: Information derived from or of value to NASA activities. Publications include final reports of major projects, monographs, data compilations, handbooks, sourcebooks, and special bibliographies.

TECHNOLOGY UTILIZATION PUBLICATIONS: Information on technology used by NASA that may be of particular interest in commercial and other non-aerospace applications. Publications include Tech Briefs, Technology Utilization Reports and Technology Surveys.

Details on the availability of these publications may be obtained from:

**SCIENTIFIC AND TECHNICAL INFORMATION OFFICE
NATIONAL AERONAUTICS AND SPACE ADMINISTRATION
Washington, D.C. 20546**